



# A HELIXOL-Derived Bisphosphinite Ligand: Synthesis and Application in Gold-Catalyzed Enynes Cycloisomerization

Caleb Medena, Francesco Calogero, Quentin Lemoine, Corinne Aubert, Etienne Derat, Louis Fensterbank, Geoffrey Gontard, Omar Abou Khaled, Nicolas Vanthuyne, Jamal Moussa, et al.

## ► To cite this version:

Caleb Medena, Francesco Calogero, Quentin Lemoine, Corinne Aubert, Etienne Derat, et al.. A HELIXOL-Derived Bisphosphinite Ligand: Synthesis and Application in Gold-Catalyzed Enynes Cycloisomerization. European Journal of Organic Chemistry, 2019, 2019 (11), pp.2129-2137. 10.1002/ejoc.201801722 . hal-02189404

**HAL Id: hal-02189404**

**<https://hal.sorbonne-universite.fr/hal-02189404>**

Submitted on 29 Aug 2019

**HAL** is a multi-disciplinary open access archive for the deposit and dissemination of scientific research documents, whether they are published or not. The documents may come from teaching and research institutions in France or abroad, or from public or private research centers.

L'archive ouverte pluridisciplinaire **HAL**, est destinée au dépôt et à la diffusion de documents scientifiques de niveau recherche, publiés ou non, émanant des établissements d'enseignement et de recherche français ou étrangers, des laboratoires publics ou privés.

# A HELIXOL-Derived Bisphosphinite Ligand: Synthesis and Application in Gold-Catalyzed Enynes Cycloisomerization

Caleb Medena,<sup>[a]</sup> Francesco Calogero,<sup>[a]</sup> Quentin Lemoine,<sup>[a]</sup> Corinne Aubert,<sup>[a]</sup> Etienne Derat,<sup>[a]</sup> Louis Fensterbank,<sup>[a]</sup> Geoffrey Gontard,<sup>[a]</sup> Omar Khaled,<sup>[a]</sup> Nicolas Vanthuyne,<sup>[b]</sup> Jamal Moussa,<sup>[a]</sup> Cyril Ollivier,<sup>[a]</sup> Marc Petit,<sup>[a]</sup> and Marion Barbazanges<sup>\*[a]</sup>

**Abstract:** The synthesis, optical resolution through derivatization, characterization, and utilization of a new helical bis(phosphinite gold) complex derived from HELIXOL are described. By using an efficient cobalt catalyst, neither irradiation nor high catalytic loading was required to access the helicene of interest.

The latter was phosphorylated to afford a new chiral ligand that was studied. Especially, treatment with AuCl(SMe<sub>2</sub>) gives a dinuclear gold complex that was used in cycloisomerization reactions.

## Introduction

Helicenes, aromatic compounds with a helical structure, intrinsically possess interesting chiroptical properties and find applications in various fields such as optics, electronics, supramolecular and organic synthesis.<sup>[1]</sup> In 2001, Reetz and Sostmann reported the first synthesis of 2,15-bishydroxy[6]helicene (HELIXOL) **1**,<sup>[2]</sup> that could be seen as a helical equivalent of BINOL (Figure 1). The authors report the resolution of both enantiomers of a cyclic precursor through preparative HPLC and used the enantio-enriched helix as an efficient fluorescent sensor for chiral amines recognition. As far as we know, in spite of two other synthetic approaches – based on photocyclization and cobalt-catalyzed [2+2+2] cycloaddition under irradiation at high temperature –<sup>[3]</sup> no other application of HELIXOL has been reported in the literature. In this work, we aimed at synthesizing,

resolving and functionalizing HELIXOL **1** to get access to a new class of helical-structured phosphinite ligand. The latter will be evaluated on efficient and versatile gold-catalyzed cycloisomerization reactions.<sup>[4]</sup>

## Results and Discussion

### Bisphosphinite Ligand Synthesis

To date, if some Co- or Ni-catalyzed [2+2+2] strategies are reported to access helicenes, they all rely on the use of a large amount of catalyst (from 20 mol-% to 50 mol-%, regarding to the catalytic system used).<sup>[5]</sup> Moreover, in addition of high catalytic loading, if nickel-catalyzed reaction can be performed at room temperature without UV- or microwave activation,<sup>[5a]</sup> use of CpCo(CO)<sub>2</sub><sup>[5a]</sup> or CpCo(CO)dmfu<sup>[5b]</sup> generally require irradiation (UV and microwaves, respectively) as well as high temperature (>140 °C). There is thus a need for new catalytic systems.

We first tested the published experimental procedure. As reported in the literature, when triyne **2** was treated with CpCo(CO)<sub>2</sub> (20 mol-%) and triphenylphosphine (40 mol-%) in decane at 140 °C under irradiation,<sup>[3b]</sup> the desired 2,15-bis-methoxy-tetrahydro[6]helicene ( $\pm$ )-**3** was isolated in 78 % yield (Table 1, entry 1). Use of air-stable CpCo(CO)dmfu (15 mol-%) under microwave irradiation and in the presence of imidazolium salt<sup>[5b]</sup> to increase the medium polarity revealed successful as **3** was isolated in 93 % yield after 15 min under microwave irradiation (Table 1, entry 2). Decreasing of the catalytic loading to 5 mol-% led to the desired tetrahydrohelicene **3** in 72 % yield due to partial conversion in spite of extended reaction time (Table 1, entry 3).

We thus turned our attention towards low-valent cobalt catalyst HCo(PMe<sub>3</sub>)<sub>4</sub>.<sup>[6]</sup> Indeed, in 2013, we disclosed the first use of HCo(PMe<sub>3</sub>)<sub>4</sub> in triynes and enediynes cycloaddition reaction.<sup>[7]</sup>

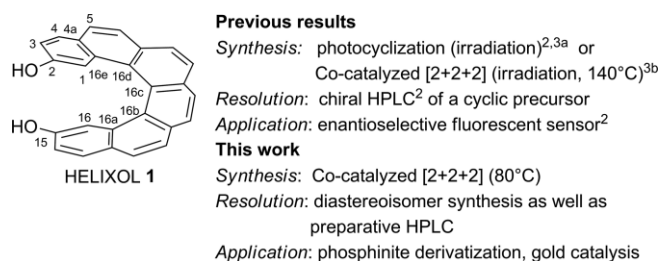
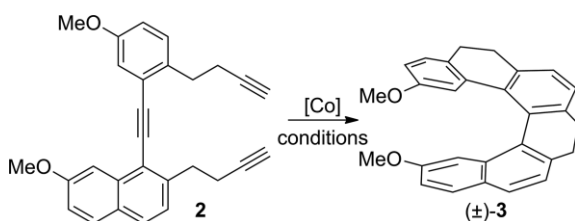


Figure 1. HELIXOL **1**.

[a] Sorbonne Université, Faculté des Sciences et Ingénierie, CNRS, Institut Parisien de Chimie Moléculaire (UMR CNRS 8232), 4 place Jussieu, 75252 Paris Cedex 05, France.  
E-mail: marion.barbazanges@sorbonne-universite.fr  
<http://www.ipcm.fr/article679.html?lang=en>

[b] Aix Marseille Univ, CNRS, Centrale Marseille, iSm2, Marseille, France

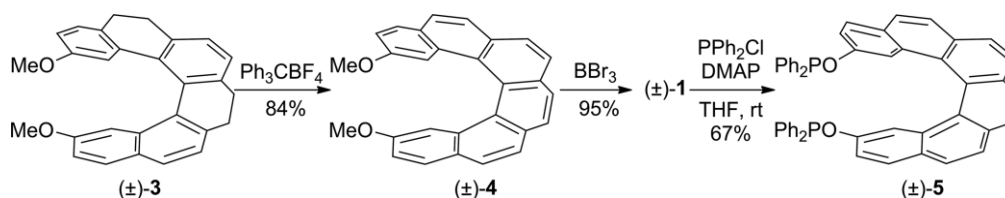
Supporting information and ORCID(s) from the author(s) for this article are available on the WWW under <https://doi.org/10.1002/ejoc.201801722>.

Table 1. Co-catalyzed [2+2+2] cycloaddition towards helical pattern ( $\pm$ )-**3**.<sup>[a]</sup>


Entries	Catalyst, x [mol-%]	Solvent, Conditions	T	Yield
1	CpCo(CO) <sub>2</sub> /PPh <sub>3</sub> , 20/40	decane, hν, 1 h 30	140 °C	78 %
2	CpCo(CO)dmfu, 15	THF/additive, MW, 15 min	170 °C	93 %
3	CpCo(CO)dmfu, 5	THF/additive, MW, 1 h	170 °C	72 %
4	HCo(PMe <sub>3</sub> ) <sub>4</sub> , 5	toluene, 24 h	80 °C	67 %

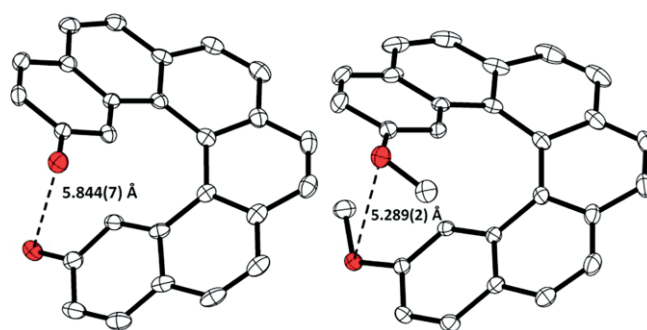
[a] Additive: [1-butyl-2,3-dimethylimidazolium][BF<sub>4</sub>] (10 mg/mL of solution).

Of particular interest was the ability of this catalyst to react at low loading and without external activation. We thus decided to extend the scope of this well-defined cobalt(I)-catalyst to more challenging helical systems. Indeed, helicity displays an amazing playground to test the new catalytic systems because of the steric hindrance of the designed helix. If no reaction occurred in THF whatever the temperature or the irradiation conditions, we had the pleasure to observe that this catalyst revealed active in toluene in the absence of irradiation. Indeed, when reacting triene **2** in the presence of 5 mol-% HCo(PMe<sub>3</sub>)<sub>4</sub> in toluene at 80 °C, ( $\pm$ )-**3** was isolated in 67 % yield (Table 1, entry 4).

Scheme 1. Bisphosphinite ( $\pm$ )-**5** synthesis.

Subsequent rearomatization and methoxy cleavage led to HELIXOL ( $\pm$ )-**1** in 80 % yield for these two steps. The latter was phosphorylated to afford the corresponding bisphosphinite ( $\pm$ )-**5** in 67 % (Scheme 1).<sup>[8]</sup> Due to bisphosphinite instability, we characterized the corresponding phosphinate ( $\pm$ )-**5=O**, obtained by direct phosphorylation with diphenylphosphinic chloride.

2,15-Bis(methoxy)helicene ( $\pm$ )-**4** was crystallized through pentane vapor diffusion in dichloromethane (Figure 2, Table 2). X-ray analysis revealed that it has an inner pitch elevation (C1...C16 distance) of 3.051(3) Å and an oxygen–oxygen distance of 5.289(2) Å. The terminal inner helix torsion angles show an unequal but relatively small opening at 10.0(3)° and 11.4(3)°. The interplanar angle of the two terminal rings is 50.85(5)°.

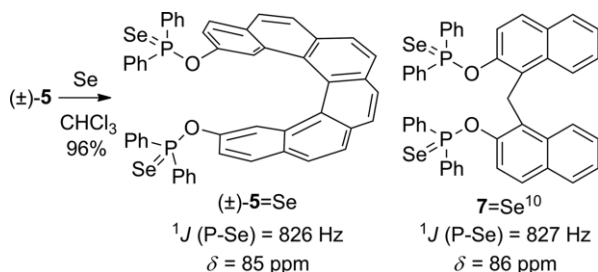
Figure 2. Molecular structures of HELIXOL ( $\pm$ )-**1** (left) and bis(methoxy)helicene ( $\pm$ )-**4** (right) with thermal ellipsoids at 30 % probability.Table 2. Main crystal data and structure refinement parameters for ( $\pm$ )-**1**, ( $\pm$ )-**4**, ( $\pm$ )-**5=Se**, (*P*)-**6** and (*M*)-**6**.

	( $\pm$ )- <b>1</b>	( $\pm$ )- <b>4</b>	( $\pm$ )- <b>5=Se</b>	( <i>P</i> )- <b>6</b>	( <i>M</i> )- <b>6</b>
Formula	C <sub>26</sub> H <sub>16</sub> O <sub>2</sub> ·H <sub>2</sub> O	C <sub>28</sub> H <sub>20</sub> O <sub>2</sub>	C <sub>50</sub> H <sub>34</sub> O <sub>2</sub> P <sub>2</sub> Se <sub>2</sub>	C <sub>50</sub> H <sub>34</sub> Au <sub>2</sub> Cl <sub>2</sub> O <sub>2</sub> P <sub>2</sub>	C <sub>50</sub> H <sub>34</sub> Au <sub>2</sub> Cl <sub>2</sub> O <sub>2</sub> P <sub>2</sub>
Formula weight	378.40	388.44	886.63	1193.54	1193.54
Crystal system	monoclinic	monoclinic	monoclinic	monoclinic	monoclinic
Space group	C 2	P 2 <sub>1</sub> /c	P 2 <sub>1</sub> /n	P 2 <sub>1</sub>	P 2 <sub>1</sub>
a	20.634(3) Å	7.7453(3) Å	16.4111(3) Å	13.4755(3) Å	13.4627(4) Å
b	7.0081(10) Å	33.3095(12) Å	9.2622(2) Å	10.1965(3) Å	10.1946(3) Å
c	12.6102(15) Å	7.6927(3) Å	27.7846(6) Å	15.3750(4) Å	15.3897(4) Å
α	90°	90°	90°	90°	90°
β	104.680(8)°	105.133(2)°	103.094(1)°	93.537(2)°	93.383(1)°
γ	90°	90°	90°	90°	90°
V	1764.0(4) Å <sup>3</sup>	1915.83(13) Å <sup>3</sup>	4113.53(15) Å <sup>3</sup>	2108.55(10) Å <sup>3</sup>	2108.51(10) Å <sup>3</sup>
Z	Z: 4 Z': 4	Z: 4 Z': 4	Z: 4 Z': 4	Z: 2 Z': 2	Z: 2 Z': 2
Temperature	200(1) K	200(1) K	200(1) K	200(1) K	200(1) K
Wavelength	1.54178 Å	1.54178 Å	0.71073 Å	1.54178 Å	1.54178 Å
Theta range	3.63° to 67.04°	5.32° to 66.59°	1.33° to 26.77°	4.24° to 66.66°	2.88° to 67.09°
Completeness	97.4 %	99.8 %	99.9 %	99.6 %	99.0 %
Flack parameter	0.5	/	/	−0.029(6)	−0.011(17)
R1 [ <i>I</i> > 2σ( <i>I</i> )]	6.09 %	4.56 %	5.71 %	2.52 %	6.64 %
wR2 (all data)	15.77 %	12.69 %	15.83 %	6.44 %	16.58 %

Racemic HELIXOL ( $\pm$ )-**1** co-crystallized with a molecule of H<sub>2</sub>O and presents a 3.173(9) Å inner pitch elevation (C1...C16 distance) and a 5.844(7) Å oxygen–oxygen distance. The terminal inner helix torsion angles show an unequal but relatively small opening at 6.4(10)° and 13.2(10)°. The interplanar angle of the two terminal rings is 60.86(17)° (Figure 2).

### Electronic Properties Evaluation

In order to evaluate its electronic properties as well as the influence of the helical cavity, phosphinite ( $\pm$ )-**5** was converted into the corresponding selenide complex ( $\pm$ )-**5**=Se (96 %) (Scheme 2).<sup>[9]</sup> The latter revealed a  $^1J_{P-Se}$  coupling constant (826 Hz) and a chemical shift (85 ppm) identical to the non-helical phosphinite **7**=Se,<sup>[10]</sup> showing that the helical cavity does not affect the phosphorus environment nor the electronic properties. These phosphinites rank in between the selenated-triphenylphosphine adduct (Se=PPh<sub>3</sub>,  $^1J_{P-Se}$  = 736 Hz) and the selenated-triphenylphosphite one (Se=P(OPh)<sub>3</sub>,  $^1J_{P-Se}$  = 1027 Hz),<sup>[11]</sup> suggesting an intermediate  $\pi$ -acidity of this ligand as expected.



Scheme 2. Selenated complexes ( $^{31}\text{P}$  NMR,  $\text{CDCl}_3$ ).

The bisphosphiniteselenide complex ( $\pm$ )-**5**=Se crystallized through pentane vapor diffusion in  $\text{CDCl}_3$ , and presents a 3.075(4) Å inner pitch elevation (C1...C16 distance) and a 5.444(4) Å oxygen–oxygen distance. The terminal inner helix torsion angles show an unequal opening at 12.8(6)° and 14.1(6)°, larger than the one observed of HELIXOL **1**. The interplanar angle of the two terminal rings is 52.45(12)° (Figure 3).

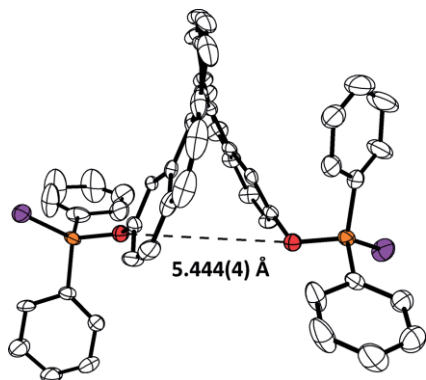
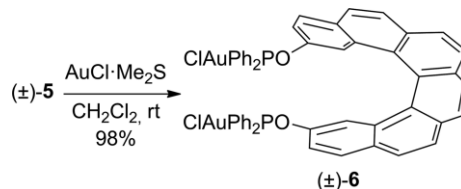


Figure 3. Molecular structure of ( $\pm$ )-**5**=Se with thermal ellipsoids at 30 % probability.

Subsequent complexation with dimethylsulfide gold chloride led to helical di-gold complex ( $\pm$ )-**6** in 98 % yield (Scheme 3).<sup>[12]</sup>

Its  $^{31}\text{P}$  NMR spectrum shows a single resonance at 112.3 ppm accounting for the two equivalent phosphinite units. The coordination shift is 4.3 ppm.



Scheme 3. Towards bisgold helical complex ( $\pm$ )-**6**.

### Bisphosphinite Ligand Evaluation in Cycloisomerization

This complex was then evaluated in enyne cycloisomerization reaction.<sup>[4]</sup> Enyne **8a** was first treated in the presence of 2 mol-% of helical bisgold complex ( $\pm$ )-**6** (ie 4 mol-% of gold atom), in the presence of a slight excess of  $\text{AgSbF}_6$  (5 mol-%) to insure cationization of the two gold moieties, in dichloromethane as the solvent. Under these conditions, the conversion was fast and total and bicyclo[4.1.0]heptene **9a** was isolated in 79 % yield after 20 min at r.t. (Table 3, entry 1). When 1 mol-% of the complex was used, partial conversion was observed and the product was isolated in 50 % yield after 3 h (entry 2). We then moved towards partial cationization of the dinuclear complex: when 0.5 equiv of silver is used per equiv of gold atom, the reaction revealed sluggish and partial conversion was observed in spite of extended reaction time (entry 3, 30 % yield, 60 % based on recovered starting material). Noteworthy, neither the gold complex nor  $\text{AgSbF}_6$  alone led to any conversion (entries 4 and 5).

Table 3. Gold-catalysed cycloisomerization.

Entries	x [mol-%]	y [mol-%]	Yield
1	2	5	79 %
2	1	2	50 %
3	2	2	30 %
4	2	0	–
5	0	5	–

Screening of the enyne partner was then achieved in the best reaction conditions ie 2 mol-% of ( $\pm$ )-**6**, 5 mol-% of  $\text{AgSbF}_6$ , in  $\text{CH}_2\text{Cl}_2$  at r.t. (Table 3, entry 1). When an *o*-nosyl electron-withdrawing group was introduced instead of the tosyl one, we had the pleasure to observe similar reactivity. Bicyclo **9b** was isolated in 89 % yield (Table 4, entry 2). Switching from a phenyl to a methyl substituent at the internal alkene position led to competition with a 5-*exo*-dig mechanism: 6-membered ring diene **10c** was formed as a by-product (19 %) along with expected product **9c** that was isolated in 69 % yield (entry 3). Introduction of an oxygen linker revealed trickier and degradation occurred. Decreasing the temperature to 0 °C allowed isola-

tion of the bicycle of interest **9d** in 40 % yield (entry 4). Finally, we performed the methoxycyclization of enyne **8e**, incorporating a diester linker and a prenyl moiety. After 1 h 30 at r.t. and in the presence of methanol as a nucleophilic co-solvent, we isolated methylenecyclopentane **12e** in 65 % yield (entry 5).

Entries	Substrate	Product (Yield)
1	<b>8a</b> R <sup>1</sup> =Ph, R <sup>2</sup> =R <sup>3</sup> =H, R <sup>4</sup> =Me, NTs X=	<b>9a</b> (79%)
2	<b>8b</b> R <sup>1</sup> =Ph, R <sup>2</sup> =R <sup>3</sup> =H, R <sup>4</sup> =Me, X=NoTs	<b>9b</b> (89%)
3	<b>8c</b> R <sup>1</sup> =Me, R <sup>2</sup> =R <sup>3</sup> =H, R <sup>4</sup> =Me, NTs X=	<b>9c</b> (69%) <b>10c</b> (19%)
4	<b>8d</b> R <sup>1</sup> =R <sup>3</sup> =H, R <sup>2</sup> =Ph, R <sup>4</sup> =pC <sub>6</sub> H <sub>4</sub> OMe, X=O	<b>9d</b> <sup>[a]</sup> (40%)
5	<b>8e</b> R <sup>1</sup> =R <sup>4</sup> =H, R <sup>2</sup> =R <sup>3</sup> =Me X=C(CO <sub>2</sub> Me) <sub>2</sub>	<b>12e</b> <sup>[b]</sup> (65%)

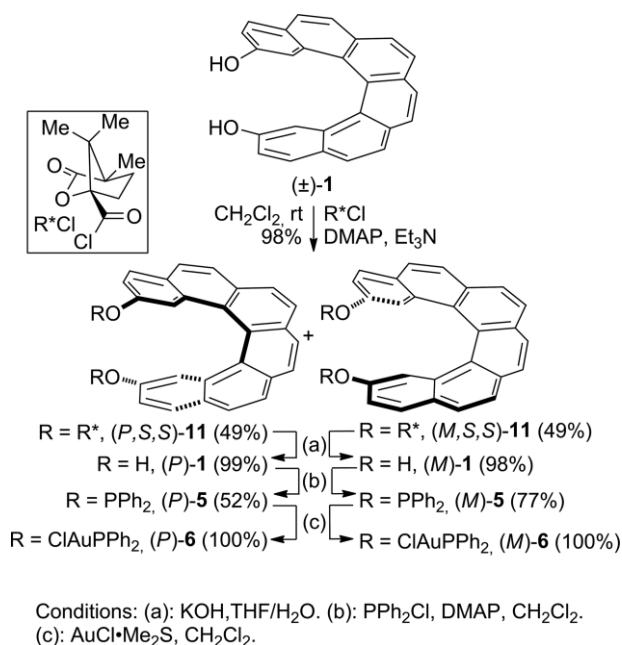
[a] The reaction was performed at 0 °C. [b] MeOH was used as co-solvent.

### Chiral Helical Phosphinite Ligand in Cycloisomerization

Next move was the evaluation of the impact of helical chirality on this cycloisomerization reaction.

First, we resolved the racemate through diastereoisomers synthesis.

Esterification of the (±)-**1** racemate with (*S,S*)-camphanic acid chloride led to a diastereomeric mixture that was separated by flash chromatography purification.<sup>[8]</sup> Subsequent saponification (KOH, THF/H<sub>2</sub>O) afforded the enantiomerically pure (ee>99 %) HELIXOLs (*P*)-**1** and (*M*)-**1** in excellent yields (48 %, 2 steps). It is worthy to note that we also developed a preparative chiral HPLC method that led to an excellent separation of both enantiomers (ee>99 %).<sup>[13]</sup> Treatment of enantiomerically pure HELIXOLs **1** by chlorodiphenylphosphine in the presence of *N,N*-dimethylaminopyridine (DMAP) led to the new helical bisphosphinite ligands (*P*)-**5** (52 %) and (*M*)-**5** (77 %) (Scheme 4).



Scheme 4. HELIXOL resolution and derivatization.

Due to bisphosphinite instability, we characterized the corresponding phosphinate **5=O**, obtained by direct phosphorylation with diphenylphosphinic chloride. The optical rotation of bisphosphinate (*P*)-**5=O** (respectively (*M*)-**5=O**) was found to be  $[\alpha]_D^{23} = +3295$  (c 0.042, CH<sub>2</sub>Cl<sub>2</sub>, 98 % ee) [respectively  $[\alpha]_D^{23} = -3829$  (c 0.040, CH<sub>2</sub>Cl<sub>2</sub>, 96 % ee)].<sup>[14]</sup> CD spectrum of (*P*)-**5=O** disclosed a broad negative band around (–)253 nm, and an intense positive band at (+)340 nm accompanied with a shoulder at 352 nm (Figure 4).

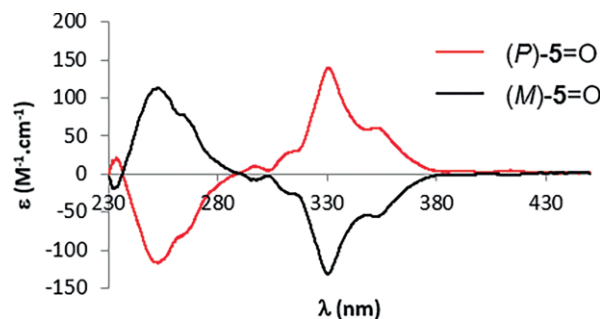


Figure 4. Bisphosphinate **5=O** CD.

CD spectrum of (*P*)-**6** is very similar to the one of bisphosphinate (*P*)-**5=O**. It discloses a broad intense negative band around (–)259 nm, and an intense positive band at (+)334 nm accompanied with a shoulder at 354 nm (Figure 5, blue line). An optical rotation of  $[\alpha]_D^{23} = +1244$  (c 0.005, CHCl<sub>3</sub>) [respectively  $[\alpha]_D^{23} = -1250$  (c 0.005, CHCl<sub>3</sub>)] was found for bisgold helix (*P*)-**6** [respectively (*M*)-**6**].

Notably, the CD spectra are in agreement with the absolute configuration determined by X-ray analysis (Table 2 and vide infra Figure 6).

(*P*)-Gold complex [respectively (*M*)-gold complex] was crystallized through pentane vapor diffusion in dichloromethane



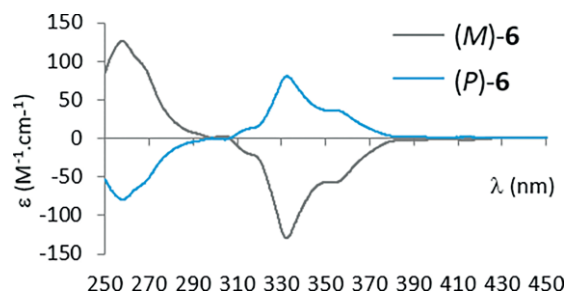


Figure 5. Gold complex **6** CD spectra.

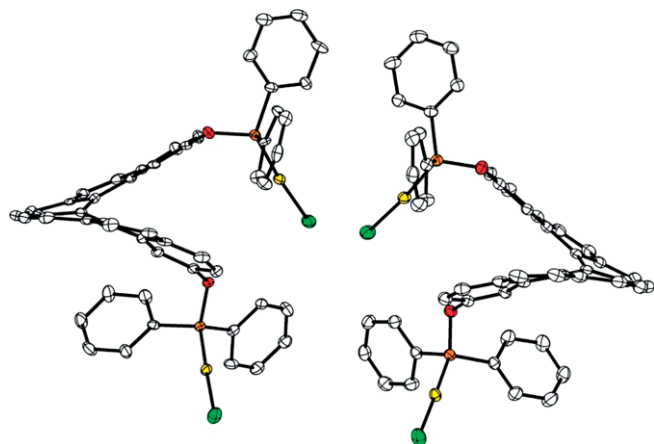


Figure 6. Molecular structures of HELIXOL bisphosphinite gold chloride complexes (*P*)-**6** (right) and (*M*)-**6** (left) with thermal ellipsoids at 30 % probability.

(Figure 6). X-ray analysis disclosed an inner pitch elevation (C1...C16 distance) of 3.111(10) Å [respectively 3.094(19) Å] and a gold–gold distance of 7.203(1) Å [respectively 7.210(1) Å], precluding any Au...Au interaction. The interplanar angle of the two terminal rings is 55.5(3)° [respectively 56.1(4)°]. Moreover, X-ray crystallography confirmed the absolute configuration attribution through circular dichroism (Table 2).

UV-Vis absorption spectra were recorded as diluted solutions in dichloromethane ( $c \approx 10^{-5}$  M) (Figure 7). As previously, accurate spectra of the free ligand **5** could not be obtained due to the high sensitivity of this molecule so the oxidized form **5=O** was studied instead.

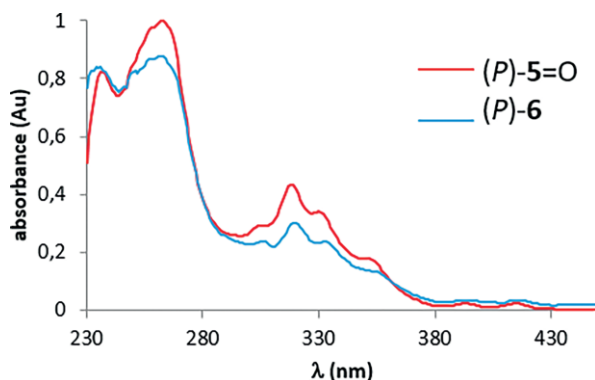


Figure 7. UV-Vis. Absorption for bisphosphinate (*P*)-**5=O** and bisgold (*P*)-**6** in dichloromethane.

The two helices (*P*)-**5=O** and (*P*)-**6** exhibited a similar pattern, with a main envelop of absorption bands in the range of 230–280 nm with high molar absorption values above  $8 \times 10^4$  M<sup>-1</sup> cm<sup>-1</sup> indicating  $\pi$ - $\pi^*$  type processes. The spectra all show several transitions in the range of 290–360 nm with lower molar absorption values ( $2$ – $4 \times 10^4$  M<sup>-1</sup> cm<sup>-1</sup>) possibly resulting from  $\pi$ - $\pi^*$  transitions and overlapping charge transfer (oxygen/AuCl moieties to the aromatic rings). We furthermore observe additional tails falling in the near UV area consistent with the presence of charge transfer processes.

Photoluminescence spectra of the oxidized form of the ligand (*P*)-**5=O** and the gold complex (*P*)-**6** were recorded in air-equilibrated dichloromethane solutions at  $c \approx 10^{-5}$  M at room temperature (Figure 8). Upon excitation around 380 nm, both compounds show strong emissions in the blue region (410–490 nm) with a structured pattern typical of oxygen/AuCl perturbed  $\pi$ - $\pi^*$  transitions. Such behavior was observed in similar helicene derived compounds.<sup>[15]</sup>

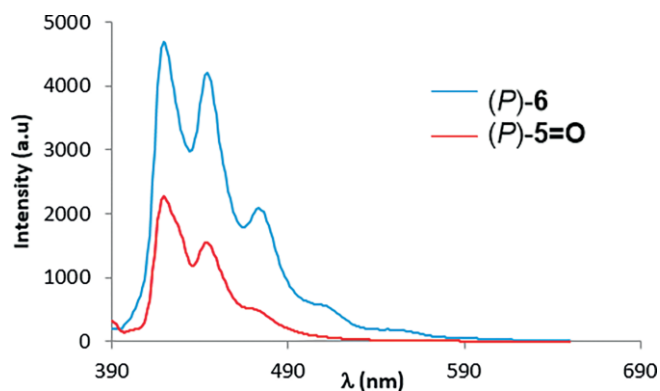
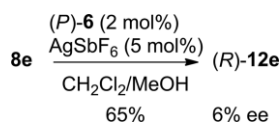


Figure 8. Photoluminescence spectra in dichloromethane solutions ( $10^{-5}$  M).

By using enantiomerically pure (*P*)-dinuclear gold pre-catalyst (*P*)-**6**, under the conditions previously optimized, no enantiomeric excess was obtained (Table 5, entry 1). To improve the ee, the temperature was decreased. When the reaction was run at 0 °C, very low enantioselectivity was observed as the bicyclo[4.1.0]heptene **9a** was obtained in 3 % ee in favor of the (*S,S*) enantiomer (entry 2).<sup>[16]</sup> Decreasing the temperature to –25 °C slowed down the reaction a lot and improved slightly the ee as (*S,S*)-**6** was formed in 11 % ee (35 % yield, entry 3). In a similar way, when enyne **8e** was cycloisomerized with (*P*)-**6** and AgSbF<sub>6</sub> in the presence of MeOH as a polar co-solvent at r.t., the desired (*R*)-methylenecyclopentane **12e** was obtained in 6 % ee (65 % yield, Scheme 5).<sup>[17]</sup>

Table 5. Cycloisomerization of enyne **8a** in the presence of chiral bisgold complex (*P*)-**6**.

$\text{8a} \xrightarrow[\text{CH}_2\text{Cl}_2]{\text{(P)-6 (2 mol-%) AgSbF}_6 \text{ (5 mol-%)}} \text{(S,S)-9a}$				
Entries	T °C	Time	Yield	ee <sup>[16]</sup>
1	25 °C	30 min	76 %	0 %
2	0 °C	75 min	65 %	3 % ( <i>S,S</i> )
3	–25 °C	1 h 30	35 %	11 % ( <i>S,S</i> )



Scheme 5. Methoxycyclization of enyne **8e** in the presence of chiral bisgold complex (*P*)-**6**.

## Conclusion

We synthesized and characterized an optically enriched new ligand bearing a helical core. Notably, by using  $\text{HCo}(\text{PMe}_3)_4$  as catalyst for the [2+2+2] cycloaddition key step, neither irradiation nor high catalytic loading was required to access HELIXOL platform. Both enantiomers of HELIXOL **1** could be isolated from diastereomeric derivatization or efficient preparative HPLC separation. The corresponding phosphinites revealed unstable and were trapped as the oxide, the selenated or the gold derivatives. The bis-gold complexes were crystallized and used to perform enynes cycloisomerization. If the racemic version revealed efficient, low enantiomeric excesses were obtained when the optically pure catalysts were tested. The low enantiomeric excesses observed are probably linked to (i) the linear geometry of gold(I) that pointed outwards from the cavity; (ii) the absence of  $\text{Au}\cdots\text{Au}$  interaction due to their distance; (iii) the helicene disubstitution in positions (2,15), so probably too far away from the helical cavity to induce chirality. Further studies will thus focus in bringing the metal center closer to the helical cavity, by switching from (2,15)-disubstitution to (1,16)-one; or by introducing sterically hindered substitution in the proxima positions. Moving towards square planar metal catalysis such as platinum- or palladium-catalysis could also lead to interesting results in asymmetric catalysis.

## Experimental Section

**General:** Unless otherwise noted, reactions were carried out in oven-dried glassware under an argon atmosphere. MeOH was dried overnight over freshly activated molecular sieves (4 Å), THF and  $\text{Et}_2\text{O}$  were distilled from sodium-benzophenone.  $\text{CH}_2\text{Cl}_2$ ,  $(\text{CH}_2\text{Cl})_2$ , pyridine,  $\text{Et}_3\text{N}$ , diisopropylamine, toluene, and benzene were distilled from  $\text{CaH}_2$ . Diphenylphosphine chloride was distilled prior to use. Other reagents and chemicals were purchased from commercial sources (Sigma-Aldrich, Alfa Aesar, Fluorochem, Strem Chemicals) and used as received. Flash chromatography was performed on silica gel Merk Geduran or DAVISIL Grace 40–63  $\mu\text{m}$ . Micro-wave assisted [2+2+2]-cycloaddition were run in microwave-type reactor, equipped with a stirring bar and sealed with a septum-cap (Biotage, n°354905). NMR spectra were recorded at room temperature on Bruker AVANCE 600, 400, or 300 spectrometers (BBFO probes), using the residual peak of chloroform (7.26 ppm for  $^1\text{H}$  NMR and 77.0 ppm for  $^{13}\text{C}$  NMR), toluene (2.08 ppm for  $^1\text{H}$  NMR and 20.4 ppm for  $^{13}\text{C}$  NMR) dichloromethane (5.32 ppm for  $^1\text{H}$  NMR and 53.84 ppm for  $^{13}\text{C}$  NMR), acetone (2.05 ppm for  $^1\text{H}$  NMR and 206.26 ppm for  $^{13}\text{C}$  NMR) or dimethyl sulfoxide (2.50 ppm for  $^1\text{H}$  NMR and 39.5 ppm for  $^{13}\text{C}$  NMR) as internal standards. Chemical shifts ( $\delta$ ) are reported in parts per million (ppm) and coupling constant (*J*) are given in Hertz (Hz).  $^1\text{H}$  and  $^{13}\text{C}$  NMR assignments were based on COSY, HSQC, HMBC experiments.  $J(\text{C-P})$  coupling constants were determined based on HSQC and HMBC experiments. Abbreviations used for peak multiplicities are: s (singlet); d (dou-

plet); t (triplet); m (multiplet, or overlap of non-equivalent resonances); High-resolution mass spectrometry was performed on a Bruker microTOF (ESI) spectrometer; Melting points (m.p.) were recorded with an SMP3 Stuart Scientific melting point apparatus. Infrared (IR) spectra were measured using Tensor 27 (ATR Diamond) Bruker spectrometer. IR data are reported as characteristic bands ( $\text{cm}^{-1}$ ) in their maximal intensity. Optical rotations were determined using a JASCO P2000. The circular dichroism was performed on a JASCO J-815 CD spectrometer equipped with a JASCO CDF-426L Peltier thermostat (2 mm quartz cell). Preparative chiral HPLC of HELIXOL was achieved on an Agilent 1260 infinity unit with pump, autosampler, oven, DAD and JASCO CD-2095 circular dichroism detector, controlled by an SRA Instrument software. Enantiomeric excesses of asymmetric catalysis were determined by using chiral HPLC Waters 2487 ( $\lambda = 254 \text{ nm}$ ).

X-ray crystal structure determination: Single crystals were selected, mounted and transferred into a cold nitrogen gas stream. Intensity data were collected with Bruker Kappa-APEX2 systems using micro-source Cu-K $\alpha$  (( $\pm$ )-**1**, ( $\pm$ )-**4**, (*P*)-**6**, (*M*)-**6**) or fine-focus sealed-tube Mo-K $\alpha$  (( $\pm$ )-**5**=Se) radiations. Unit-cell parameters determination, data collection strategy, integration, and absorption correction were carried out with the Bruker APEX2 suite of programs. The structures were solved with SHELXT-2014 and refined anisotropically by full-matrix least-squares methods with SHELXL-2014 using the WinGX suite (( $\pm$ )-**1**, ( $\pm$ )-**4**, (*P*)-**6**, (*M*)-**6**) or Olex2 (( $\pm$ )-**5**=Se). Compound ( $\pm$ )-**1** was refined as a perfect inversion twin. Absolute structures of (*P*)-**6** and (*M*)-**6** were determined by anomalous scattering effects analysis and their chemical absolute configurations were then deduced.

CCDC 1819308 (for ( $\pm$ )-**1**), 1819309 (for ( $\pm$ )-**4**), 1872217 (for ( $\pm$ )-**5**=Se), 1819310 for (*P*)-**6** and 1819311 (for (*M*)-**6**) contain the supplementary crystallographic data for this paper. These data can be obtained free of charge from The Cambridge Crystallographic Data Centre.

**Crystal data for ( $\pm$ )-1.**  $\text{C}_{26}\text{H}_{18}\text{O}_3$ , monoclinic C 2,  $a = 20.634(3) \text{ \AA}$ ,  $b = 7.0081(10) \text{ \AA}$ ,  $c = 12.6102(15) \text{ \AA}$ ,  $\alpha = \gamma = 90^\circ$ ,  $\beta = 104.680(8)^\circ$ ,  $V = 1764.0(4) \text{ \AA}^3$ ,  $Z = 4$ , colourless prism  $0.05 \times 0.05 \times 0.02 \text{ mm}^3$ ,  $\mu = 0.740 \text{ mm}^{-1}$ , min/max transmission = 0.71/0.86,  $T = 200(1) \text{ K}$ ,  $\lambda = 1.54178 \text{ \AA}$ ,  $\theta$  range =  $3.63^\circ$  to  $67.04^\circ$ , 5034 reflections measured, 2698 independent,  $R_{\text{int}} = 0.0931$ , completeness = 0.974, 264 parameters, 1 restraints, Flack  $x = 0.5$ , final R indices  $R1 [I > 2\sigma(I)] = 0.0609$  and  $wR2$  (all data) = 0.1577, GOF on  $F^2 = 0.981$ , largest difference peak/hole =  $0.20/-0.26 \text{ e \AA}^{-3}$ .

**Crystal data for ( $\pm$ )-4.**  $\text{C}_{28}\text{H}_{20}\text{O}_2$ , monoclinic  $P21/c$ ,  $a = 7.7453(3) \text{ \AA}$ ,  $b = 33.3095(12) \text{ \AA}$ ,  $c = 7.6927(3) \text{ \AA}$ ,  $\alpha = \gamma = 90^\circ$ ,  $\beta = 105.133(2)^\circ$ ,  $V = 1915.83(13) \text{ \AA}^3$ ,  $Z = 4$ , pale yellow prism  $0.33 \times 0.11 \times 0.08 \text{ mm}^3$ ,  $\mu = 0.655 \text{ mm}^{-1}$ , min/max transmission = 0.83/0.93,  $T = 200(1) \text{ K}$ ,  $\lambda = 1.54178 \text{ \AA}$ ,  $\theta$  range =  $5.32^\circ$  to  $66.59^\circ$ , 16518 reflections measured, 3384 independent,  $R_{\text{int}} = 0.0728$ , completeness = 0.998, 274 parameters, 0 restraints, final R indices  $R1 [I > 2\sigma(I)] = 0.0456$  and  $wR2$  (all data) = 0.1269, GOF on  $F^2 = 1.055$ , largest difference peak/hole =  $0.19/-0.19 \text{ e \AA}^{-3}$ .

**Crystal data for ( $\pm$ )-5=Se.**  $\text{C}_{50}\text{H}_{34}\text{O}_2\text{P}_2\text{Se}_2$ , monoclinic  $P 2_1/n$ ,  $a = 16.4111(3) \text{ \AA}$ ,  $b = 9.2622(2) \text{ \AA}$ ,  $c = 27.7846(6) \text{ \AA}$ ,  $\alpha = \gamma = 90^\circ$ ,  $\beta = 103.094(1)^\circ$ ,  $V = 4113.53(15) \text{ \AA}^3$ ,  $Z = 4$ , colourless plate  $0.08 \times 0.19 \times 0.20 \text{ mm}^3$ ,  $\mu = 1.916 \text{ mm}^{-1}$ , min/max transmission = 0.75/0.91,  $T = 200(1) \text{ K}$ ,  $\lambda = 0.71073 \text{ \AA}$ ,  $\theta$  range =  $1.33^\circ$  to  $26.77^\circ$ , 28443 reflections measured, 8769 independent,  $R_{\text{int}} = 0.0285$ , completeness = 0.999, 595 parameters, 76 restraints, final R indices  $R1 [I > 2\sigma(I)] = 0.0571$  and  $wR2$  (all data) = 0.1583, GOF on  $F^2 = 1.042$ , largest difference peak/hole =  $1.09/-0.55 \text{ e \AA}^{-3}$ .

**Crystal data for (P)-6.**  $C_{50}H_{34}Au_2Cl_2O_2P_2$ , monoclinic  $P\ 2_1$ ,  $a = 13.4755(3)\ \text{\AA}$ ,  $b = 10.1965(3)\ \text{\AA}$ ,  $c = 15.3750(4)\ \text{\AA}$ ,  $\alpha = \gamma = 90^\circ$ ,  $\beta = 93.537(2)^\circ$ ,  $V = 2108.55(10)\ \text{\AA}^3$ ,  $Z = 2$ , yellow prism  $0.35 \times 0.05 \times 0.05\ \text{mm}^3$ ,  $\mu = 15.097\ \text{mm}^{-1}$ , min/max transmission = 0.20/0.61,  $T = 200(1)\ \text{K}$ ,  $\lambda = 1.54178\ \text{\AA}$ ,  $\theta$  range =  $4.24^\circ$  to  $66.66^\circ$ , 25456 reflections measured, 7327 independent,  $R_{\text{int}} = 0.0426$ , completeness = 0.996, 523 parameters, 1 restraint, Flack  $x = -0.029(6)$ , final R indices  $R_1 [I > 2\sigma(I)] = 0.0252$  and  $wR_2$  (all data) = 0.0644, GOF on  $F^2 = 1.049$ , largest difference peak/hole =  $0.80/-0.52\ \text{e}\ \text{\AA}^{-3}$ .

**Crystal data for (M)-6.**  $C_{50}H_{34}Au_2Cl_2O_2P_2$ , monoclinic  $P\ 2_1$ ,  $a = 13.4627(4)\ \text{\AA}$ ,  $b = 10.1946(3)\ \text{\AA}$ ,  $c = 15.3897(4)\ \text{\AA}$ ,  $\alpha = \gamma = 90^\circ$ ,  $\beta = 93.383(1)^\circ$ ,  $V = 2108.51(10)\ \text{\AA}^3$ ,  $Z = 2$ , yellow prism  $0.9 \times 0.3 \times 0.1\ \text{mm}^3$ ,  $\mu = 15.097\ \text{mm}^{-1}$ , min/max transmission = 0.02/0.32,  $T = 200(1)\ \text{K}$ ,  $\lambda = 1.54178\ \text{\AA}$ ,  $\theta$  range =  $2.88^\circ$  to  $67.09^\circ$ , 25983 reflections measured, 7420 independent,  $R_{\text{int}} = 0.0442$ , completeness = 0.990, 524 parameters, 1 restraints, Flack  $x = -0.011(17)$ , final R indices  $R_1 [I > 2\sigma(I)] = 0.0664$  and  $wR_2$  (all data) = 0.1658, GOF on  $F^2 = 1.041$ , largest difference peak/hole =  $2.18/-2.52\ \text{e}\ \text{\AA}^{-3}$ .

**UV-Vis. absorption and emission properties:** Unless otherwise stated, all measurements of the UV-Vis absorption and emission spectra were performed at 298 K and in distilled dichloromethane solutions. UV-Vis. spectra were recorded on a JASCO V-670 Spectrometer. Photoluminescence spectra were recorded using a JASCO J-815 CD Spectrometer.

**Synthetic procedures:** Triyne **2** was synthesized through the procedure described in the literature,<sup>[3b]</sup> as well as enynes **8a**,<sup>[18]</sup> **8b**,<sup>[19]</sup> **8c**,<sup>[18]</sup> **8d**,<sup>[20]</sup> **8e**.<sup>[21]</sup>

#### Tetrahydrohelicene ( $\pm$ )-3:

**Procedure for Table 1, entry 1:**<sup>[3b]</sup> In a Schlenk flask, to a solution of triyne **2** (524 mg, 1.33 mmol, 1 equiv) and triphenylphosphine (139 mg, 532  $\mu\text{mol}$ , 0.4 equiv) in degassed *n*-decane (0.05 M, 33 mL) at  $90^\circ\text{C}$ , was added  $\text{CpCo}(\text{CO})_2$  (36  $\mu\text{L}$ , 265  $\mu\text{mol}$ , 0.2 equiv). The mixture was stirred at  $140^\circ\text{C}$  for 2 h under concomitant irradiation with a halogen lamp. The solvent was removed under reduced pressure and the residue was purified by flash chromatography on silica gel (petroleum ether/ $\text{Et}_2\text{O}$ , 98/2), to yield tetrahydrohelicene ( $\pm$ )-**3** (411 mg, 78 %) as a yellow solid. Characterization data are in agreement with those previously reported in the literature.<sup>[3b]</sup>

**Procedure for Table 1, entry 2:** In a microwave reactor, to a solution of triyne **2** (31.3 mg, 0.080 mmol, 1 equiv) and imidazolium salt (50 mg) in THF (5 mL) was added  $\text{CpCo}(\text{CO})\text{dmfu}$  (3.5 mg, 12  $\mu\text{mol}$ , 0.15 equiv) and the vial was sealed. After degassing by argon bubbling (10 min) through the septum, the mixture was heated at  $170^\circ\text{C}$  under microwave irradiation. After 15 min, the vial was cooled to room temperature, and the reaction mixture concentrated under reduced pressure. The residue was purified by flash chromatography on silica gel (petroleum ether/ $\text{Et}_2\text{O}$ , 98/2), to yield tetrahydrohelicene ( $\pm$ )-**3** (29 mg, 93 %) as a yellow solid.

**Procedure for Table 1, entry 3:** In a microwave reactor, to a solution of triyne **2** (31.3 mg, 0.080 mmol, 1 equiv) and imidazolium salt (50 mg) in THF (5 mL) was added  $\text{CpCo}(\text{CO})\text{dmfu}$  (1.2 mg, 4.0  $\mu\text{mol}$ , 0.05 equiv) and the vial was sealed. After degassing by argon bubbling (10 min) through the septum, the mixture was heated at  $170^\circ\text{C}$  under microwave irradiation. After 1 h, the vial was cooled to room temperature and the reaction mixture concentrated under reduced pressure. The residue was purified by flash chromatography on silica gel (petroleum ether/ $\text{Et}_2\text{O}$ , 98/2), to yield tetrahydrohelicene ( $\pm$ )-**3** (22.4 mg, 72 %) as a yellow solid.

**Procedure for Table 1, entry 4:** To a solution of  $\text{HCo}(\text{PMe}_3)_4$  (2.7 mg, 0.01 mmol, 0.05 equiv) in toluene (0.5 mL) was added a solution of

triyne **2** (50 mg, 0.13 mmol, 1 equiv) in toluene (2.0 mL). After 18 h at  $80^\circ\text{C}$ , the reaction mixture was concentrated under reduced pressure. Purification by flash chromatography on silica gel gave ( $\pm$ )-**3** (34 mg, 67 %) as a yellow solid.

**Dimethoxyhelicene ( $\pm$ )-4:** To a solution of tetrahydrohelicene ( $\pm$ )-**3** (389 mg, 990  $\mu\text{mol}$ , 1 equiv) in 1,2-dichloroethane (25 mL) was added  $\text{Ph}_3\text{CBF}_4$  (980 mg, 2.97 mmol, 3 equiv). The mixture was stirred at  $80^\circ\text{C}$  for 18 h. Evaporation of the solvent and purification by flash chromatography on silica gel (petroleum ether/ $\text{Et}_2\text{O}$ , 95:5) afforded dimethoxyhelicene ( $\pm$ )-**4** (323 mg, 84 %) as a yellow solid. The latter was crystallized through pentane vapor diffusion in dichloromethane. Characterization data are in agreement with those previously reported in the literature.<sup>[3b]</sup>

**HELIXOL ( $\pm$ )-1:** To a solution of dimethoxyhelicene ( $\pm$ )-**4** (312 mg, 803  $\mu\text{mol}$ , 1 equiv) in dichloromethane (27 mL) at  $0^\circ\text{C}$  was slowly added  $\text{BBr}_3$  (1 M in  $\text{CH}_2\text{Cl}_2$ , 8.03 mL, 8.03 mmol, 10 equiv). After 18 h at r.t., the reaction mixture was quenched with water, and the separated aqueous layer was extracted with dichloromethane. The combined organic extracts were dried with anhydrous  $\text{MgSO}_4$  and concentrated under reduced pressure. The residue was purified by chromatography on silica gel (petroleum ether/ $\text{EtOAc}$ , 80:20) to afford the HELIXOL ( $\pm$ )-**1** (275 mg, 95 %) as a yellow solid. The latter was crystallized by slow evaporation of  $\text{CD}_2\text{Cl}_2$ . Characterization data are in agreement with those previously reported in the literature.<sup>[3b]</sup>

#### HELIXOL Optical Resolution:

**(*P,S,S*)-2,15-bis{4',7',7'-trimethyl-3'-oxo-2'-oxabicyclo[2.2.1]heptane-1'-carbonyloxy}[6]helicene ((*P,S,S*)-11) and (*M,S,S*)-2,15-bis{4',7',7'-trimethyl-3'-oxo-2'-oxabicyclo[2.2.1]heptane-1'-carbonyloxy}[6]helicene ((*M,S,S*)-11):** To a solution of ( $\pm$ )-**1** (364 mg, 1.01 mmol, 1 equiv), DMAP (123 mg, 1.01 mmol, 1 equiv) and  $\text{Et}_3\text{N}$  (0.56 mL, 4.04 mmol, 4 equiv) in dichloromethane (28 mL) at  $0^\circ\text{C}$  was added a solution of (1S)-(-)-camphanic acid chloride (656 mg, 3.03 mmol, 3 equiv) in dichloromethane (7 mL). After 18 h at r.t., the solvent was evaporated under reduced pressure and the residue purified by flash chromatography on silica gel (petroleum ether/ $\text{EtOAc}$ : 80:20 to 70:30) to afford (*P,S,S*)-**11** (early eluting fraction) as a brown solid (349 mg, 49 %) and (*M,S,S*)-**11** (late eluting fraction) as a brown solid (350 mg, 49 %).

**(*P,S,S*)-11:**  $[\alpha]_D^{23} = +1808$  ( $c = 0.005$ ,  $\text{CHCl}_3$ ); HRMS (ESI)  $m/z$  calcd. for  $\text{C}_{46}\text{H}_{40}\text{O}_8$  ( $[\text{M} + \text{Na}]^+$ ): 743.2615, found 743.2625. IR (neat):  $\nu$  ( $\text{cm}^{-1}$ ) = 3045, 2968, 2934, 2876, 1780, 1766, 1309, 1256, 1218, 1168, 1106, 1046, 852, 758;  $R_f = 0.51$  (petroleum ether/ $\text{EtOAc}$ : 60:40);  $^1\text{H NMR}$  (400 MHz,  $\text{CDCl}_3$ )  $\delta$  0.85 (s, 6H), 0.90 (s, 6H), 1.13 (s, 6H), 1.67 (ddd,  $J = 13.2, 8.8, 4.2\ \text{Hz}$ , 2H), 1.85–1.98 (m, 4H), 2.37 (ddd,  $J = 12.6, 10.2, 4.2\ \text{Hz}$ , 2H), 7.11 (dd,  $J = 8.7, 2.4\ \text{Hz}$ , 2H), 7.35 (d,  $J = 2.4\ \text{Hz}$ , 2H), 7.82 (d,  $J = 8.7\ \text{Hz}$ , 2H), 7.85 (d,  $J = 8.5\ \text{Hz}$ , 2H), 7.92 (d,  $J = 8.5\ \text{Hz}$ , 2H), 7.98 (d,  $J = 8.2\ \text{Hz}$ , 2H), 8.02 (d,  $J = 8.2\ \text{Hz}$ , 2H).  $^{13}\text{C NMR}$  (100 MHz,  $\text{CDCl}_3$ )  $\delta$  9.7 (2CH<sub>3</sub>), 16.7 (2CH<sub>3</sub>), 16.8 (2CH<sub>3</sub>), 28.8 (2CH<sub>2</sub>), 30.3 (2CH<sub>2</sub>), 54.4 (2C), 54.7 (2C), 90.6 (2C), 118.8 (2CH), 120.2 (2CH), 123.8 (C), 126.5 (2CH), 126.9 (2C), 127.2 (2CH), 127.4 (2CH), 127.6 (2CH), 129.0 (2CH), 129.9 (2C), 130.4 (2C), 131.8 (2C), 133.2 (C), 147.5 (2C), 165.2 (2C), 177.8 (2C).

**(*M,S,S*)-11:**  $[\alpha]_D^{23} = -1802$  ( $c = 0.005$ ,  $\text{CHCl}_3$ ); HRMS (ESI)  $m/z$  calcd. for  $\text{C}_{46}\text{H}_{40}\text{O}_8$  ( $[\text{M} + \text{Na}]^+$ ): 743.2615, found 743.2625;  $R_f = 0.45$  (petroleum ether/ $\text{EtOAc}$ : 60:40);  $^1\text{H NMR}$  (400 MHz,  $\text{CDCl}_3$ )  $\delta$  0.77 (s, 6H), 0.95 (s, 6H), 1.13 (s, 6H), 1.70 (ddd,  $J = 13.2, 9.2, 4.2\ \text{Hz}$ , 2H), 2.05–1.89 (m, 4H), 2.37 (ddd,  $J = 13.2, 4.2, 2.6\ \text{Hz}$ , 2H), 7.09 (dd,  $J = 8.7, 2.3\ \text{Hz}$ , 2H), 7.34 (d,  $J = 2.3\ \text{Hz}$ , 2H), 7.81 (d,  $J = 8.7\ \text{Hz}$ , 2H), 7.85 (d,  $J = 8.6\ \text{Hz}$ , 2H), 7.93 (d,  $J = 8.6\ \text{Hz}$ , 2H), 7.97 (d,  $J = 8.2\ \text{Hz}$ , 2H), 8.02 (d,  $J = 8.2\ \text{Hz}$ , 2H);  $^{13}\text{C NMR}$  (100 MHz,  $\text{CDCl}_3$ )  $\delta$  9.6 (2CH<sub>3</sub>), 16.7



(2CH<sub>3</sub>), 16.9 (2CH<sub>3</sub>), 28.9 (2CH<sub>2</sub>), 30.5 (2CH<sub>2</sub>), 54.3 (2C), 54.7 (2C), 90.6 (2C), 119.0 (2CH), 120.2 (2CH), 123.7 (C), 126.6 (2CH), 126.9 (2C), 127.2 (2CH), 127.5 (2CH), 127.6 (2CH), 129.0 (2CH), 129.9 (2C), 130.5 (2C), 131.8 (2C), 133.25 (C), 147.3 (2C), 165.3 (2C), 177.6 (2C).

To a solution of (*P,S,S*)-**11** (299 mg, 0.41 mmol, 1 equiv) in THF (20 mL) at 0 °C was added a solution of KOH (233 mg, 4.15 mmol, 10 equiv) in H<sub>2</sub>O (20 mL). After 2 h at r.t., the reaction mixture was quenched with acetic acid (1 mL) and diluted with CH<sub>2</sub>Cl<sub>2</sub>. The separated aqueous phase was extracted with CH<sub>2</sub>Cl<sub>2</sub>, and the combined organic extracts were washed with a saturated aqueous solution of NaHCO<sub>3</sub>, then dried with MgSO<sub>4</sub>, filtered and concentrated under reduced pressure. The residue was purified by flash chromatography on silica gel (petroleum ether/EtOAc, 80:20) to give (*P*)-**1** as a yellow solid (148 mg, 99 %).

Similarly, HELIXOL (*M*)-**1** was obtained from (*M,S,S*)-**11** (0.20 g, 0.28 mmol) in THF (14 mL) and KOH (0.16 g, 2.8 mmol, 10 equiv) in water (14 mL). Purification by flash chromatography on silica gel (petroleum ether/EtOAc, 80:20) led to (*M*)-**1** (99 mg, 98 %) as a yellow solid.

Chiral HPLC analysis were realized on Column ChiralPak IA, hexanes/*i*PrOH: 67:33 flow rate 1 mL/min, λ = 254 nm: 6.06 min (*P*), and 21.46 min (*M*).

**Representative procedure for bisphosphinite 5:** To a solution of HELIXOL (±)-**1** (51 mg, 0.14 mmol, 1 equiv) in THF (degassed by argon bubbling, 1.5 mL) were successively added a solution of *N,N*-dimethyl-4-aminopyridine (55 mg, 0.43 mmol, 3 equiv) in THF (degassed by argon bubbling, 1 mL) then chlorodiphenylphosphine (0.10 mL, 0.56 mmol, 4 equiv). After 18 h at r.t., the solvent was removed in vacuo and the residue was purified by flash chromatography on basic alumina (hexanes/EtOAc/Et<sub>3</sub>N: 90:10:10) to afford phosphinite (±)-**5** as a yellow solid (69 mg, 67 %). *R*<sub>f</sub>: 0.65 (petroleum ether/EtOAc: 80:20 on aluminum oxide neutral); *HRMS* (*ESI*) *m/z* Calcd. for C<sub>50</sub>H<sub>34</sub>O<sub>2</sub>P<sub>2</sub> ([M + K]<sup>+</sup>): 767.1671, found 767.1685; *IR* (*neat*): ν (cm<sup>-1</sup>) = 3056, 3016, 1434, 1555, 1474, 1432, 1247, 1090, 1007, 840, 815, 793, 749, 698; <sup>1</sup>H NMR (400 MHz, CD<sub>2</sub>Cl<sub>2</sub>) δ 7.03 (app. br d, *J* = 8.5, 2H), 7.38–7.24 (m, 20H), 7.49 (app. t, *J* = 2.7 Hz, 2H), 7.56 (d, *J* = 8.7 Hz, 2H), 7.80 (d, *J* = 8.5 Hz, 2H), 7.86 (d, *J* = 8.5 Hz, 2H), 7.97 (d, *J* = 8.2 Hz, 2H), 8.00 (d, *J* = 8.2 Hz, 2H); <sup>31</sup>P NMR (162 MHz, CD<sub>2</sub>Cl<sub>2</sub>): δ 108.04.

**Selenated complex (±)-5=Se:** To a solution of (±)-**5** (24.9 mg, 0.034 mmol, 1 equiv) in CHCl<sub>3</sub> (1 mL) was added Selenium (22.8 mg, 0.29 mmol, 8.5 equiv). After 18 h at 80 °C, the reaction mixture was filtered over Celite (CHCl<sub>3</sub>) then concentrated in vacuo to afford (±)-**5=Se** (28.9 mg, 96 %) as a yellow solid; *melting point*: 245–250 °C (decomposed); *HRMS* (*ESI*) *m/z* Calcd. for C<sub>50</sub>H<sub>34</sub>O<sub>2</sub>P<sub>2</sub>Se<sub>2</sub> ([M+Na]<sup>+</sup>): 911, 0269, found 911.0277; *IR* (*neat*): ν (cm<sup>-1</sup>) = 3049, 2963, 2920, 2852, 2360, 2332 1256, 1102, 1015, 804, 700, 648; <sup>1</sup>H NMR (400 MHz, CDCl<sub>3</sub>) δ 7.19 (ddd, *J* = 8.6, 2.4, 1.3 Hz, 2H), 7.28–7.22 (m, 6H), 7.32–7.37 (m, 2H), 7.53–7.42 (m, 10H), 7.72 (app. d, *J* = 8.7 Hz, 2H), 7.75 (d, *J* = 8.5 Hz, 2H), 7.79 (d, *J* = 8.7 Hz, 2H), 7.88 (d, *J* = 8.2 Hz, 2H), 7.90 (d, *J* = 8.2 Hz, 2H), 7.91 (d, *J* = 8.2 Hz, 2H), 7.95 (d, *J* = 8.2 Hz, 2H); <sup>13</sup>C NMR (101 MHz, CDCl<sub>3</sub>) δ 119.8 (d, *J*<sub>C-P</sub> = 5.6 Hz, 2CH), 121.2 (d, *J*<sub>C-P</sub> = 4.3 Hz, 2CH), 124.0 (C), 126.1 (2CH), 126.8 (2C), 127.1 (4CH), 127.4 (2CH), 128.2 (d, *J*<sub>metaC-P</sub> = 13.7 Hz, 4CH), 128.3 (2CH), 128.4 (d, *J*<sub>metaC-P</sub> = 13.6 Hz, 4CH), 129.2 (d, *J*<sub>C-P</sub> = 1.6 Hz, 2C), 130.6 (d, *J*<sub>C-P</sub> = 1.6 Hz, 2C), 131.0 (d, *J*<sub>orthoC-P</sub> = 7.8 Hz, 4CH), 131.2 (d, *J*<sub>orthoC-P</sub> = 7.8 Hz, 4CH), 131.6 (d, *J*<sub>paraC-P</sub> = 3.1 Hz, 2CH), 131.7 (2C), 131.9 (d, *J*<sub>paraC-P</sub> = 3.2 Hz, 2CH), 133.9 (d, *J*<sub>ipsoC-P</sub> = 173.3 Hz, 2C<sub>Ph</sub>), 133.6 (C), 134.7 (d, *J*<sub>ipsoC-P</sub> = 177.4 Hz, 2C<sub>Ph</sub>), 148.3 (d, *J*<sub>C-P</sub> = 9.0 Hz, 2C-O-P) (complex NMR due to <sup>31</sup>P/<sup>13</sup>C coupling); <sup>31</sup>P NMR (162 MHz, CDCl<sub>3</sub>) δ 85 (d, <sup>1</sup>*J*<sub>P-Se</sub> = 826 Hz).

**Representative procedure for bisphosphinite 5=O:** To a suspension of NaH (42 mg, 60 % in mineral oil, 1.01 mmol, 2.5 equiv) in THF (1 mL) was added a solution of HELIXOL (±)-**1** (150 mg, 0.42 mmol, 1 equiv) in THF (1 mL). After 15 min at r.t., the reaction mixture was cooled down to 0 °C and diphenylphosphinite chloride (0.19 mL, 1.01 mmol, 2.5 equiv) was slowly added. After 15 min at 0 °C then 3 h at r.t., the reaction mixture was quenched at 0 °C with water (5 mL) and Et<sub>2</sub>O (5 mL). The aqueous layer was extracted with Et<sub>2</sub>O then the combined organic extracts were washed with and once with brine, dried with Na<sub>2</sub>SO<sub>4</sub> then concentrated under reduced pressure. The residue was purified by flash chromatography on silica gel (99:1= CH<sub>2</sub>Cl<sub>2</sub>/MeOH) to yield **5=O** (194 mg, 61 %) as a yellow solid. *HRMS* (*ESI*) *m/z* Calcd. for C<sub>50</sub>H<sub>34</sub>O<sub>4</sub>P<sub>2</sub> ([M+Na]<sup>+</sup>): 783.1825, found 783.1828; *melting point*: 110 °C; *IR* (*neat*): ν (cm<sup>-1</sup>) = 3058, 2923, 2850, 1604, 1507, 1477, 1232, 1181, 1128, 1110, 1022, 980, 927, 884, 751, 728, 692, 610, 574, 544, 528; <sup>1</sup>H NMR (400 MHz, CDCl<sub>3</sub>) δ 7.22 (apparent br td, *J* = 7.6, 3.6 Hz, 4H), 7.32–7.27 (m, 2H), 7.37–7.33 (m, 4H), 7.52–7.39 (m, 10H), 7.65–7.54 (m, 4H), 7.73 (d, *J* = 8.7 Hz, 2H), 7.87 (br s, 4H), 7.91 (d, AB syst., *J* = 8.2 Hz, 2H), 7.94 (d, AB syst., *J* = 8.2 Hz, 2H); <sup>13</sup>C NMR (100 MHz, CDCl<sub>3</sub>) δ <sup>13</sup>C NMR (100 MHz, CDCl<sub>3</sub>) δ 118.1 (d, *J*<sub>C-P</sub> = 6.1 Hz, 2CH), 119.7 (d, *J*<sub>C-P</sub> = 3.8 Hz, 2CH), 124.0 (C), 125.9 (2CH), 126.8 (2C), 127.1 (2CH), 127.2 (2CH), 127.3 (2CH), 128.3 (d, *J*<sub>metaC-P</sub> = 13.5 Hz, 4CH), 128.5 (d, *J*<sub>metaC-P</sub> = 13.5 Hz, 4CH), 128.9 (2CH), 129.0 (2C), 130.7 (d, *J*<sub>ipsoC-P</sub> = 137.9 Hz, 2C), 130.9 (2C), 131.1 (d, *J*<sub>ipsoC-P</sub> = 138.8 Hz, 2C), 131.4 (d, *J*<sub>orthoC-P</sub> = 10.4 Hz, 4CH), 131.5 (d, *J*<sub>orthoC-P</sub> = 10.4 Hz, 4CH), 131.8 (2C), 132.0 (d, *J*<sub>paraC-P</sub> = 2.8 Hz, 2CH), 132.2 (d, *J*<sub>paraC-P</sub> = 2.9 Hz, 2CH), 132.9 (C), 148.3 (d, *J*<sub>C-P</sub> = 8.6 Hz, 2CH) (complex NMR due to <sup>31</sup>P/<sup>13</sup>C coupling); <sup>31</sup>P NMR (121 MHz, CDCl<sub>3</sub>) δ = 29.6 ppm; (*P*)-**5=O**: [α]<sub>D</sub><sup>23</sup> = +3295 (c = 0.042, CH<sub>2</sub>Cl<sub>2</sub>, 98 %ee); (*M*)-**5=O**: [α]<sub>D</sub><sup>23</sup> = -3829 (c = 0.040, CH<sub>2</sub>Cl<sub>2</sub>, 96 %ee).<sup>[14]</sup>

**Representative procedure to access gold complex 6:** To a solution of (*P*)-**5** (73 mg, 0.10 mmol, 1 equiv) in CH<sub>2</sub>Cl<sub>2</sub> (20 mL) was added AuCl(Me<sub>2</sub>S) (62 mg, 0.21 mmol, 2.1 equiv). After 18 h at r.t., the reaction mixture was concentrated under reducer pressure. The residue was dissolved in dichloromethane and purified by precipitation with pentane to obtain (*P*)-**6** (119 mg, quant.) as a white solid. The complex was crystallized by diffusion of pentane into the solution of product in CH<sub>2</sub>Cl<sub>2</sub> to afford colorless crystal. *Melting point*: 245–250 °C (decomposed); *HRMS* (*ESI*) *m/z* calcd. for C<sub>50</sub>H<sub>34</sub>Au<sub>2</sub>ClO<sub>2</sub>P<sub>2</sub> ([M - Cl]<sup>+</sup>): 1157.1054, found 1157.1010; Calcd for C<sub>50</sub>H<sub>34</sub>Au<sub>2</sub>O<sub>2</sub>P<sub>2</sub> ([M - AuCl<sub>2</sub>]<sup>+</sup>): 925.1694, found 925.1720; *IR* (*neat*): ν (cm<sup>-1</sup>) = 3038, 2920, 2845, 1607, 1428, 1166, 1105, 908, 847, 746, 645; <sup>1</sup>H NMR (400 MHz, CD<sub>2</sub>Cl<sub>2</sub>) δ 7.33–7.28 (m, 4H), 7.45–7.39 (m, 4H), 7.64–7.48 (m, 16H), 7.70 (d, *J* = 8.3 Hz, 2H), 7.73 (d, *J* = 8.6 Hz, 2H), 7.89 (d, *J* = 8.6 Hz, 2H), 7.99 (d, *J* = 8.3 Hz, 2H), 8.04 (d, *J* = 8.3 Hz, 2H); <sup>13</sup>C NMR (150 MHz, CD<sub>2</sub>Cl<sub>2</sub>) δ 118.7 (d, *J*<sub>C-P</sub> = 6.4 Hz, 2CH), 121.0 (d, *J*<sub>C-P</sub> = 5.9 Hz, 2CH), 124.3 (C), 126.9 (2CH), 127.1 (2C), 127.9 (2CH), 128.0 (2CH), 128.2 (2CH), 129.68 (d, *J*<sub>C-P</sub> = 12.9 Hz, 4CH), 129.69 (d, *J*<sub>C-P</sub> = 12.6 Hz, 4CH), 129.9 (2C), 130.4 (2CH), 131.2 (2C), 132.2 (d, *J*<sub>C-P</sub> = 16.3 Hz, 4CH), 132.5 (2C), 132.6 (d, *J*<sub>C-P</sub> = 16.3 Hz, 4CH), 133.2 (d, *J*<sub>C-P</sub> = 2.5 Hz, 2CH), 133.3 (d, *J*<sub>C-P</sub> = 2.5 Hz, 2CH), 133.5 (d, *J*<sub>C-P</sub> = 71.0 Hz, 2CH), 133.6 (d, *J*<sub>C-P</sub> = 70.0 Hz, 2C), 133.7 (C), 152.2 (d, *J*<sub>C-P</sub> = 5.5 Hz, 2C) (complex NMR due to <sup>31</sup>P/<sup>13</sup>C coupling); <sup>31</sup>P NMR (162 MHz, CDCl<sub>3</sub>) δ 112.3 (s). (*P*)-**6**: [α]<sub>D</sub><sup>23</sup> = +1244 (c = 0.005, CHCl<sub>3</sub>); (*M*)-**6**: [α]<sub>D</sub><sup>23</sup> = -1250 (c = 0.005, CHCl<sub>3</sub>).

**Representative procedure for enyne 8 cycloisomerization:** To a solution of bis-gold complex **6** (x equiv) in CH<sub>2</sub>Cl<sub>2</sub> was added AgSbF<sub>6</sub> (y equiv). After 5 min at r.t., AgCl precipitation was observed. The reaction mixture was cooled to 0 °C and a solution of 1,6-enyne **8** (1 equiv) in CH<sub>2</sub>Cl<sub>2</sub> (final concentration 0.05 M) was added then the reaction mixture was stirred at room temperature. After completion, the reaction was quenched with Et<sub>3</sub>N, then fil-

tered through a short pad of Celite® (CH<sub>2</sub>Cl<sub>2</sub>) and concentrated in vacuo. The residue was purified by flash chromatography on silica gel to afford the cyclic product **9** which spectroscopic description matched the data reported in the literature.

## Acknowledgments

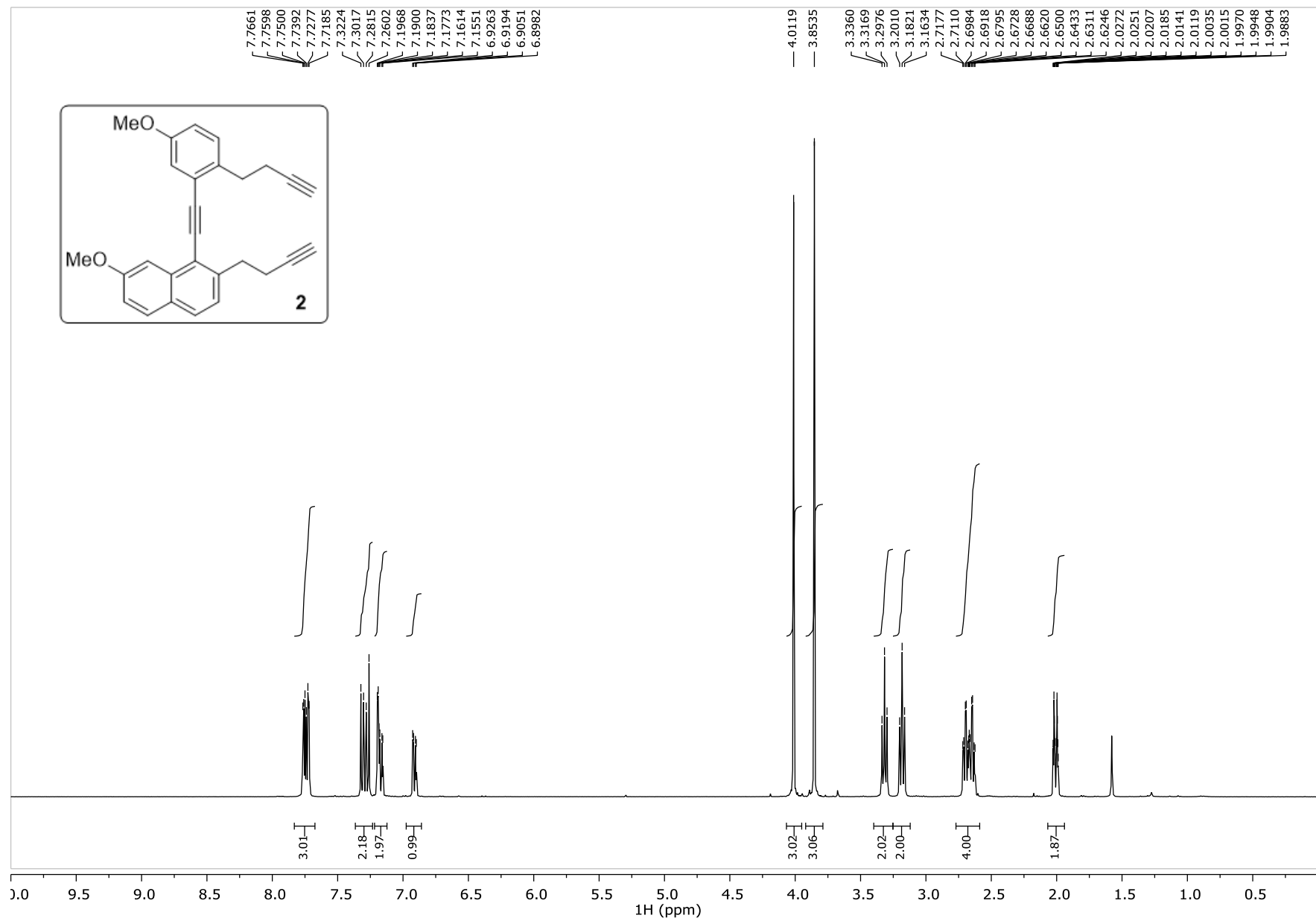
This work was supported by the CNRS, Sorbonne Université, IUF and Agence Nationale de la Recherche (ANR-13-JS07-0013-HELcats). We warmly thank D. Marquez, S. Queric, S. Zhang and C. Fagnan for precursor synthesis, J. Forté for X-ray structure of (±)-**5**=Se and Dr. A. Voituriez for fruitful discussions.

**Keywords:** Helicene · Phosphinite · Homogeneous catalysis · Chirality · Enyne Cycloisomerization

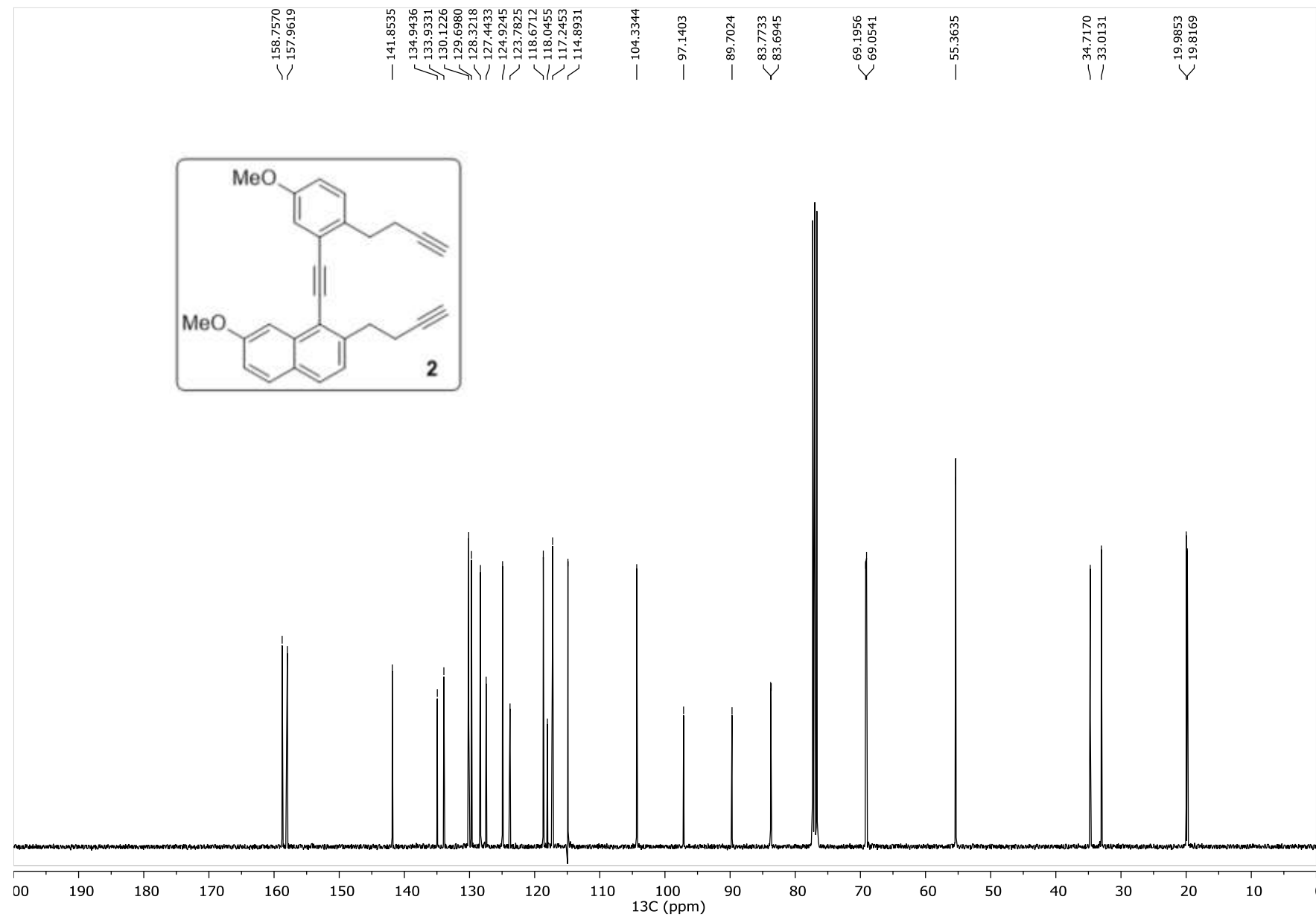
- [1] For recent reviews and book, see: a) C.-F. Chen, Y. Shen, *Helicene Chemistry*, Springer-Verlag Berlin Heidelberg, **2017**; b) N. Saleh, C. Shen, J. Crassous, *Chem. Sci.* **2014**, *5*, 3680–3694; c) P. Aillard, A. Voituriez, A. Marinetti, *Dalton Trans.* **2014**, *43*, 15263–15278; d) M. J. Narcis, N. Takenaka, *Eur. J. Org. Chem.* **2014**, *2014*, 21–34; e) Y. Shen, C.-F. Chen, *Chem. Rev.* **2012**, *112*, 1463–1535; f) M. Gingras, *Chem. Soc. Rev.* **2013**, *42*, 1051–1095.
- [2] M. T. Reetz, S. Sostmann, *Tetrahedron* **2001**, *57*, 2515–2520.
- [3] *Photocyclization*: a) C. Wachsmann, E. Weber, M. Czugler, W. Seichter, *Eur. J. Org. Chem.* **2003**, *2003*, 2863–2876; *[2+2+2] cycloaddition*: b) F. Teplý, I. G. Stará, I. Starý, A. Kollárovič, D. Luštinec, Z. Krausová, D. Šaman, P. Fiedler, *Eur. J. Org. Chem.* **2007**, *2007*, 4244–4250.
- [4] a) Reviews on gold catalyzed cycloisomerization: C. Aubert, L. Fensterbank, P. Garcia, M. Malacria, A. Simonneau, *Chem. Rev.* **2011**, *111*, 1954–1993; b) M. Rudolph, A. S. K. Hashmi, *Chem. Soc. Rev.* **2012**, *41*, 2448–2462; c) W. Yang, A. S. K. Hashmi, *Chem. Soc. Rev.* **2014**, *43*, 2941–2955; d) Y.-M. Wang, A. D. Lackner, F. D. Toste, *Acc. Chem. Res.* **2014**, *47*, 889–901; e) C. Obradors, A. M. Echavarren, *Chem. Commun.* **2014**, *50*, 16–28; f) A. Fürstner, *Acc. Chem. Res.* **2014**, *47*, 925–938.
- [5] a) I. G. Stará, I. Starý, A. Kollárovič, F. Teplý, Š. Vyskočil, D. Šaman, *Tetrahedron Lett.* **1999**, *40*, 1993–1996; b) M. Šámal, S. Chercheja, J. Rybáček, J. V. Chocholoušová, J. Vacek, L. Bednarova, D. Šaman, I. G. Stará, I. Starý, *J. Am. Chem. Soc.* **2015**, *137*, 8469–8474.
- [6] H. F. Klein, *Angew. Chem. Int. Ed. Engl.* **1970**, *9*, 904–904; *Angew. Chem.* **1970**, *82*, 885–886.
- [7] S. Ventre, C. Simon, F. Rekhroukh, M. Malacria, M. Amatore, C. Aubert, M. Petit, *Chem. Eur. J.* **2013**, *19*, 5830–5835.
- [8] A unique example of phosphinite held on a helical scaffold was reported in the literature, see: T. Tsujihara, N. Inado-Nozaki, T. Takehara, D. Y. Zhou, T. Suzuki, T. Kawano, *Eur. J. Org. Chem.* **2016**, 4948–4952.
- [9] a) D. W. Allen, L. A. March, I. W. Nowell, *J. Chem. Soc., Dalton Trans.* **1984**, 483–485; b) D. W. Allen, B. F. Taylor, *J. Chem. Soc., Dalton Trans.* **1982**, 51–54.
- [10] M. S. Balakrishna, R. Panda, J. T. Mague, *J. Chem. Soc., Dalton Trans.* **2002**, 4617–4621.
- [11] C. Glidewell, E. J. Leslie, *J. Chem. Soc., Dalton Trans.* **1977**, 527–531.
- [12] For previous gold complexes bearing a helical core and their use in catalysis, see: a) K. Yavari, P. Aillard, Y. Zhang, F. Nuter, P. Retailleau, A. Voituriez, A. Marinetti, *Angew. Chem. Int. Ed.* **2014**, *53*, 861–865; *Angew. Chem.* **2014**, *126*, 880–884; b) K. Yavari, P. Retailleau, A. Voituriez, A. Marinetti, *Chem. Eur. J.* **2013**, *19*, 9939–9947; c) S. Cauteruccio, A. Loos, A. Bossi, M. C. B. Jaimes, D. Dova, F. Rominger, S. Prager, A. Dreuw, E. Licandro, A. S. K. Hashmi, *Inorg. Chem.* **2013**, *52*, 7995–8004; d) P. Aillard, A. Voituriez, D. Dova, S. Cauteruccio, E. Licandro, A. Marinetti, *Chem. Eur. J.* **2014**, *20*, 12373–12376; e) P. Aillard, P. Retailleau, A. Voituriez, A. Marinetti, *Chem. Eur. J.* **2015**, *21*, 11989–11993.
- [13] HPLC conditions: Chiralpak IA (250 × 10 mm), hexane/ethanol/chloroform (20:40:40), flow-rate = 5 mL/min, UV detection at 280 nm. Retention times: 3.34 ((P)-**1**, ee>99.5) and 4.82 ((M)-**1**, ee>99.5).
- [14] ee were determined via chiral HPLC, conditions: Chiralpak IF (250 × 4.6 mm, 5 microns), heptane/ethanol/dichloromethane (5:3:2), flow-rate = 1 mL/min, UV detection at 254 nm and polarimetric detection (Jasco OR-1590), Retention times: (P)-**5**=O = 7.2 min, (M)-**5**=O = 13.0 min, see supporting information. The difference in optical rotation probably arose from hydration, as bisphosphinates are highly hygroscopic.
- [15] L. Norel, M. Rudolph, N. Vanthuyne, J. A. G. Williams, C. Lescop, C. Rousset, J. Autschbach, J. Crassous, R. Réau, *Angew. Chem. Int. Ed.* **2010**, *49*, 99–102; *Angew. Chem.* **2010**, *122*, 103–106.
- [16] ee was determined by using a Chiralpak AS-H Column, 98:2 *n*-hexane/*i*PrOH, 1 mL/min. Retention time for major enantiomer: 52.54 min; for minor enantiomer: 65.46 min. Attribution of the absolute configuration was done in agreement with the data published in the literature, see: P. Zhang, C. Tugny, J. M. Suarez, M. Guitet, E. Derat, N. Vanthuyne, Y. Zhang, O. Bistri, V. Mouries-Mansuy, M. Menand, *Chem* **2017**, *3*, 174–191.
- [17] ee was determined by using a Chiralpak AD-H column (95:5 *n*-hexanes/*i*PrOH, 1 mL/min): Retention time for minor enantiomer: 5.58 min; for major enantiomer: 6.57 min. Attribution of the absolute configuration was done in agreement with the data published in the literature, see: a) K.-i. Yamada, Y. Matsumoto, K. B. Selim, Y. Yamamoto, K. Tomioka, *Tetrahedron* **2012**, *68*, 4159–4165; b) M. P. Muñoz, J. Adrio, J. C. Carretero, A. M. Echavarren, *Organometallics* **2005**, *24*, 1293–1300.
- [18] T. Shibata, Y. Kobayashi, S. Maekawa, N. Toshida, K. Takagi, *Tetrahedron* **2005**, *61*, 9018–9024.
- [19] M. Barbazanges, M. Auge, J. Moussa, H. Amouri, C. Aubert, C. Desmarests, L. Fensterbank, V. Gandon, M. Malacria, C. Ollivier, *Chem. Eur. J.* **2011**, *17*, 13789–13794.
- [20] T. Kudoh, T. Mori, M. Shirahama, M. Yamada, T. Ishikawa, S. Saito, H. Kobayashi, *J. Am. Chem. Soc.* **2007**, *129*, 4939–4947.
- [21] F. Schröder, C. Tugny, E. Salanouve, H. Clavier, L. Giordano, D. Moraleda, Y. Gimbert, V. Mouries-Mansuy, J.-P. Goddard, L. Fensterbank, *Organometallics* **2014**, *33*, 4051–4056.

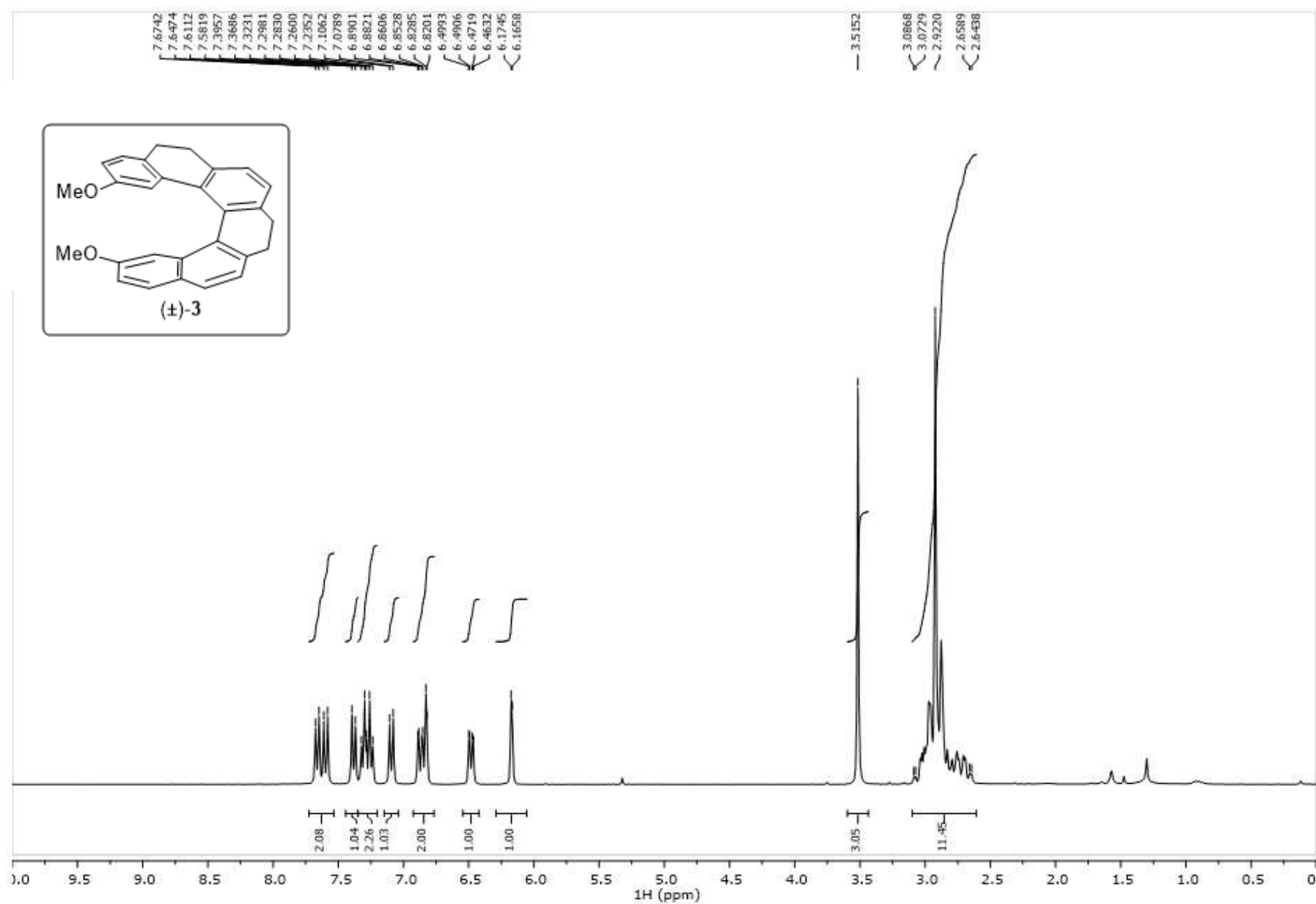
# Supporting information

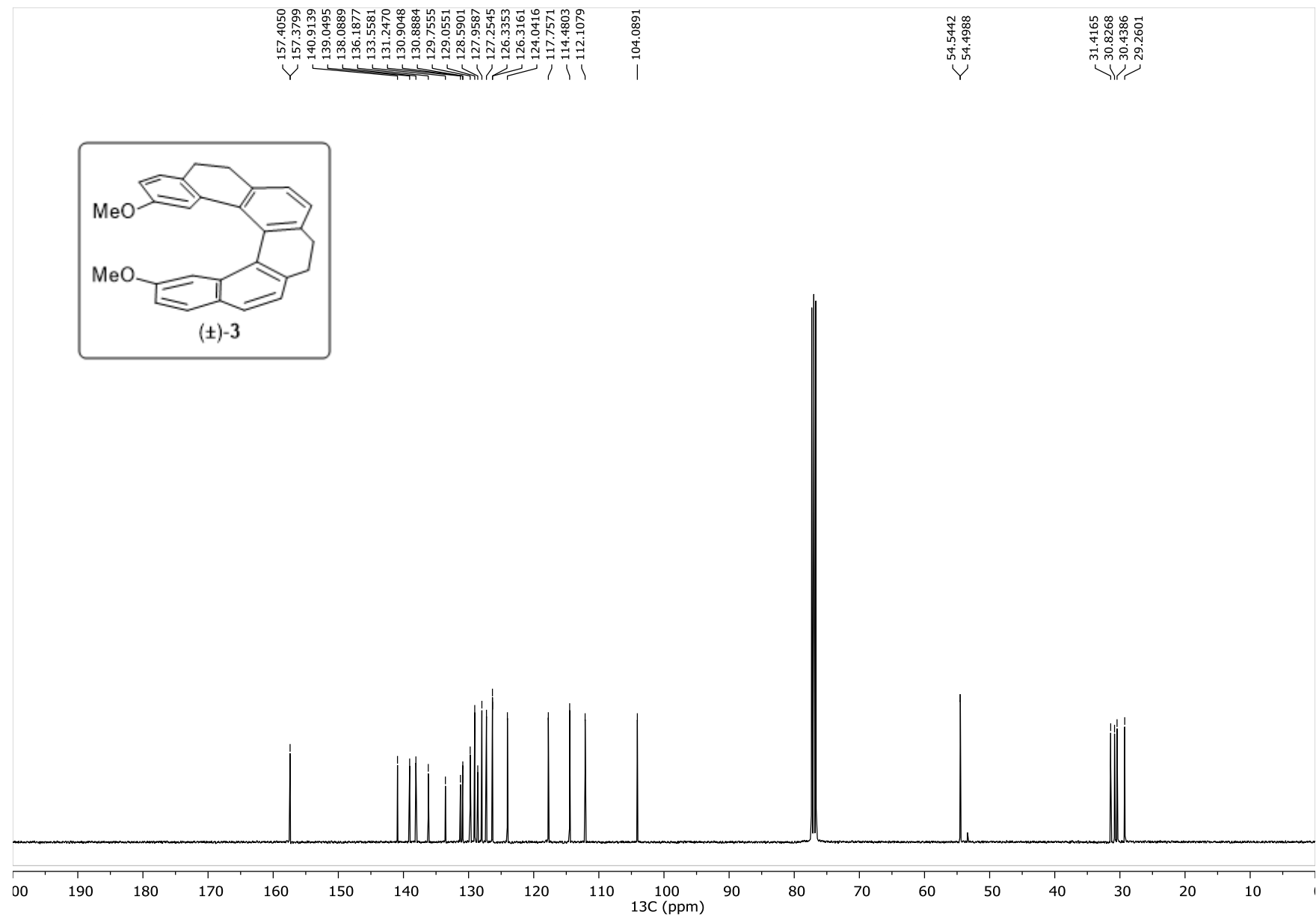
- 1) NMR spectra ( $^1\text{H}$ ,  $^{13}\text{C}$ ,  $^{31}\text{P}$ ) of precursor **2** and helical structures **1**, **3**, **4**, **5=Se**, **5=O**, **6** (*M,S,S*)-**11** and (*P,S,S*)-**11**.....S-2
- 2) Bisphosphinate **5=O** chiral HPLC analysis .....S-23
- 3) Asymmetric catalysis: HPLC traces .....S-25
- 4)  $^1\text{H}$  and  $^{13}\text{C}$  spectra of cycloisomerization products .....S-30

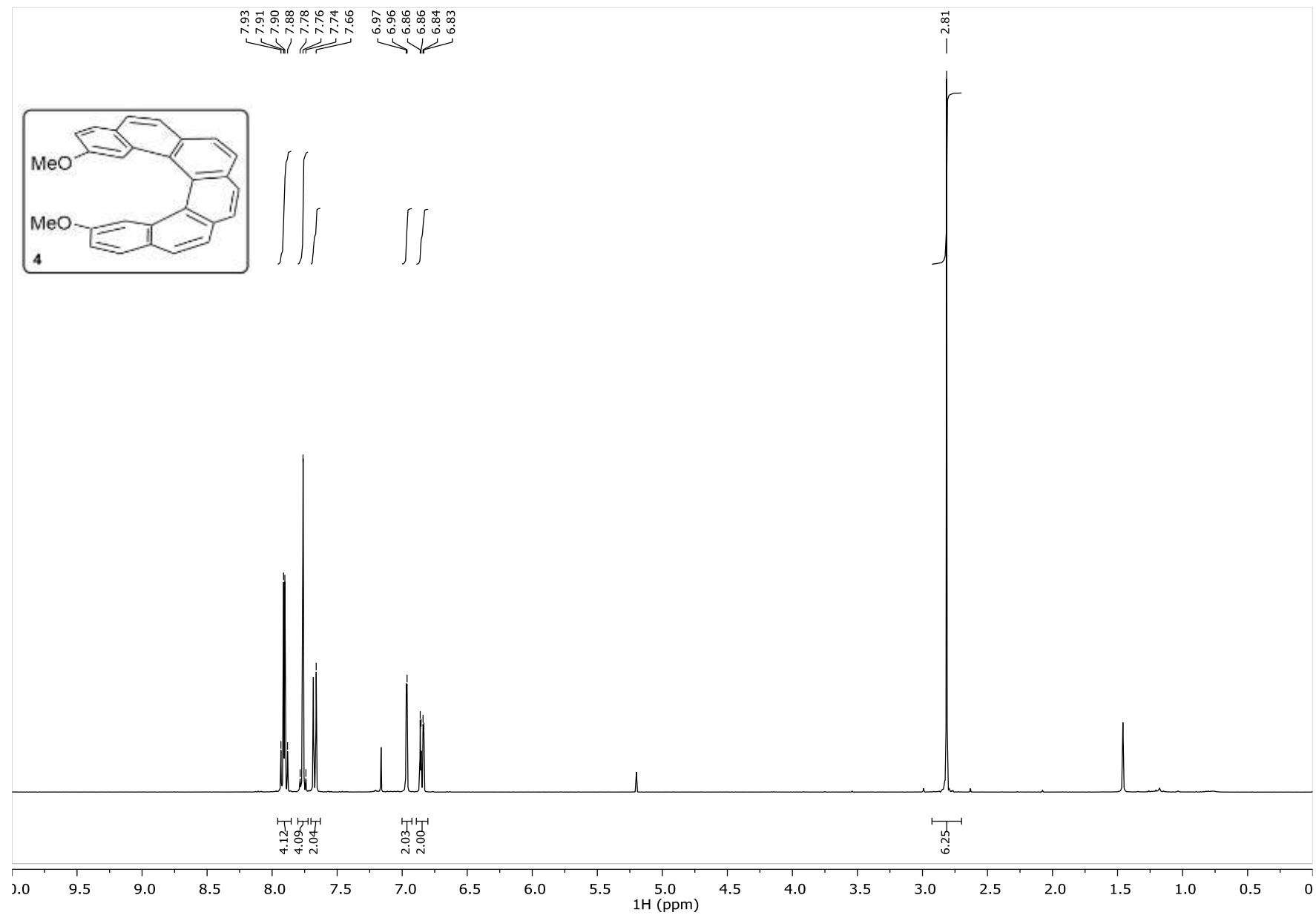




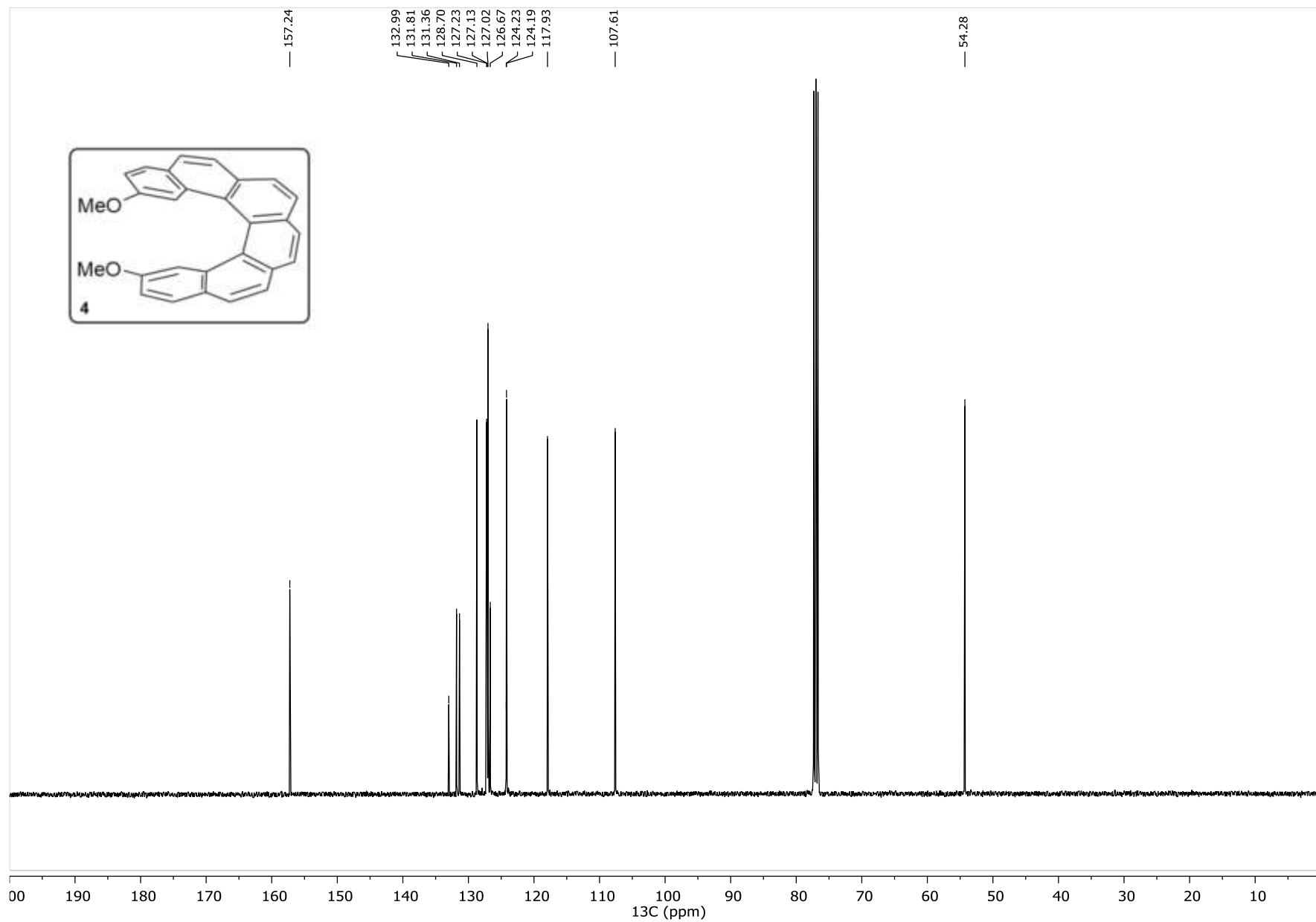


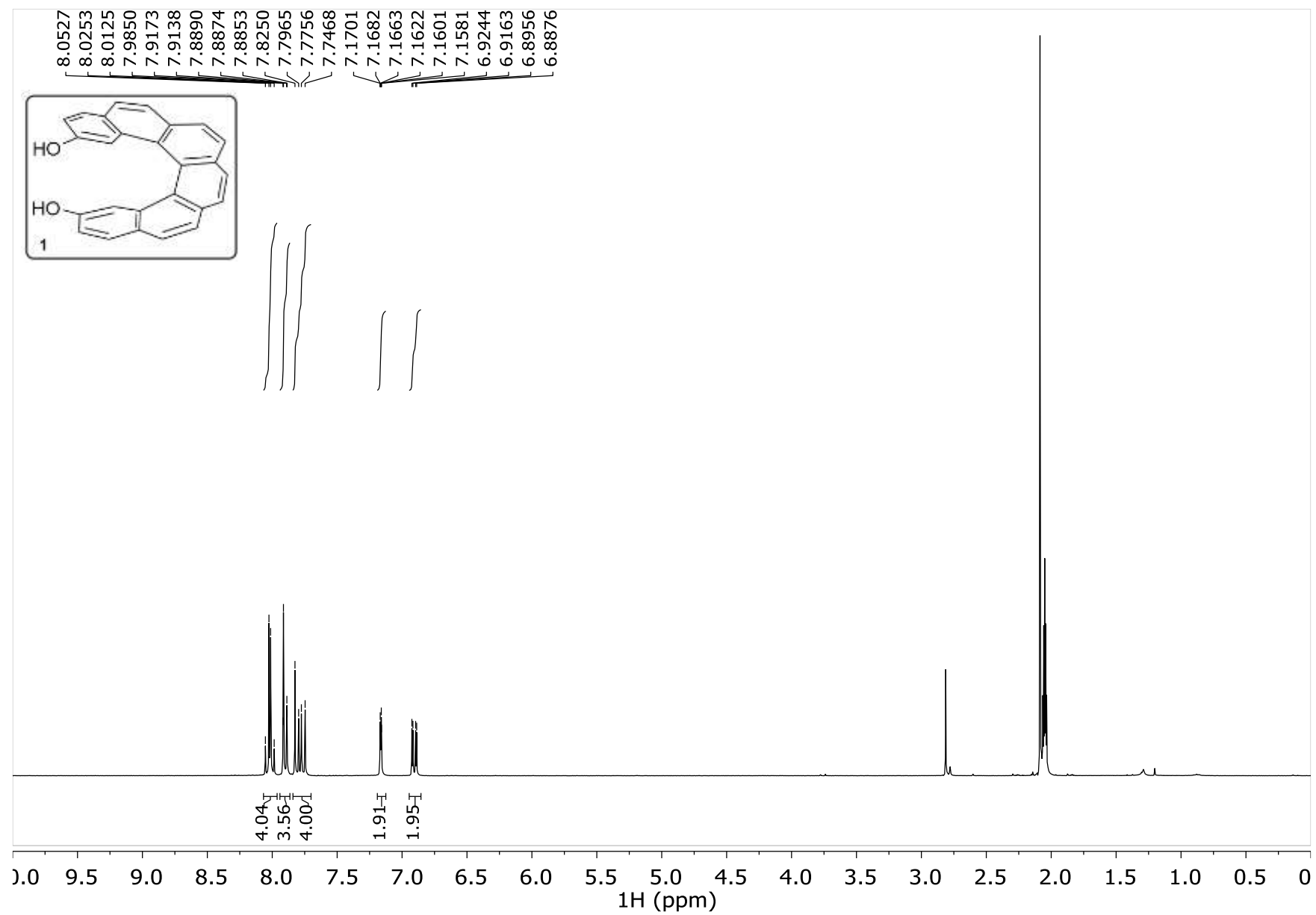


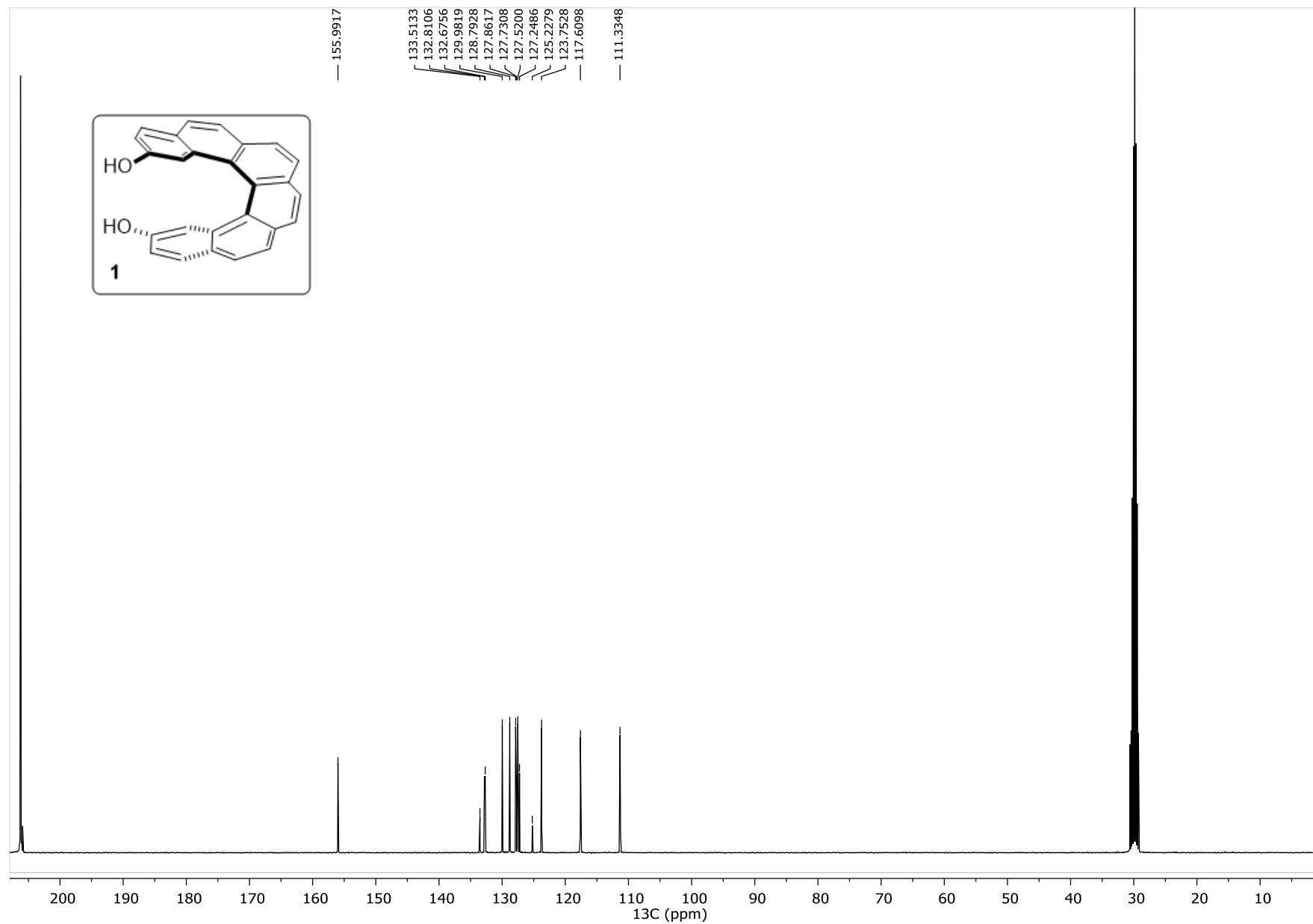


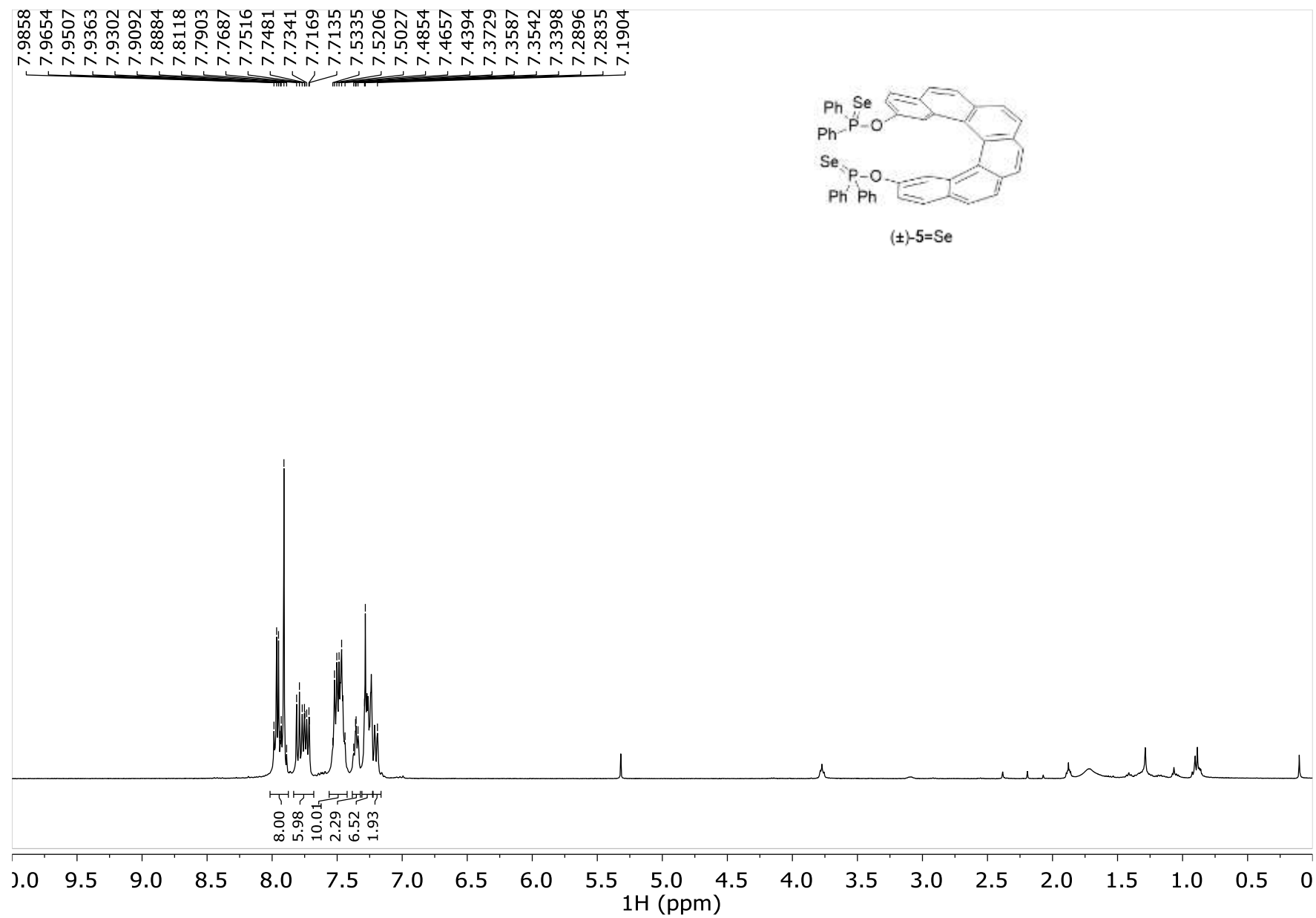




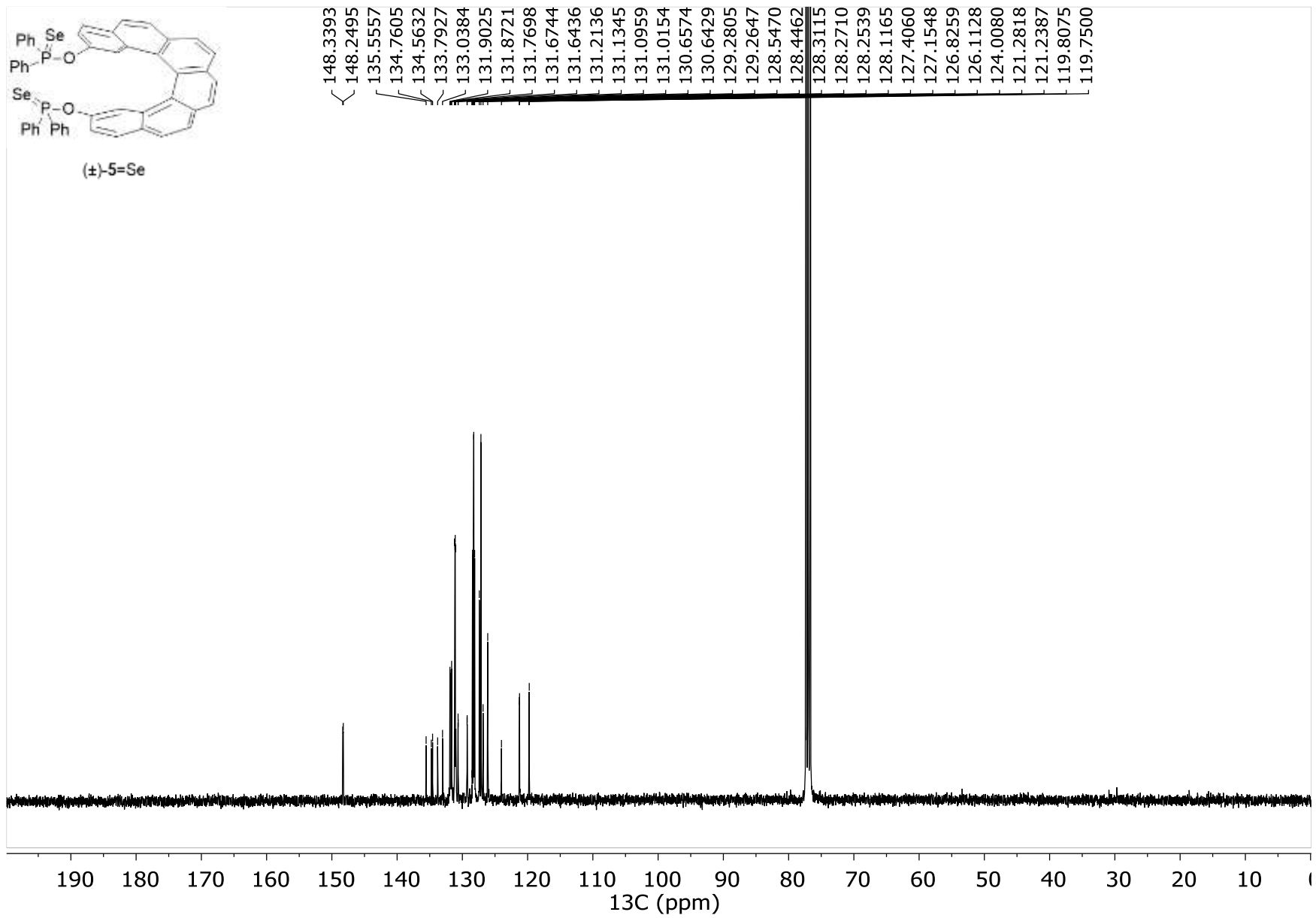


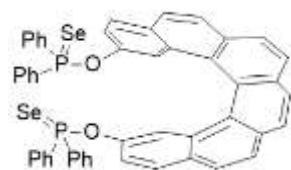




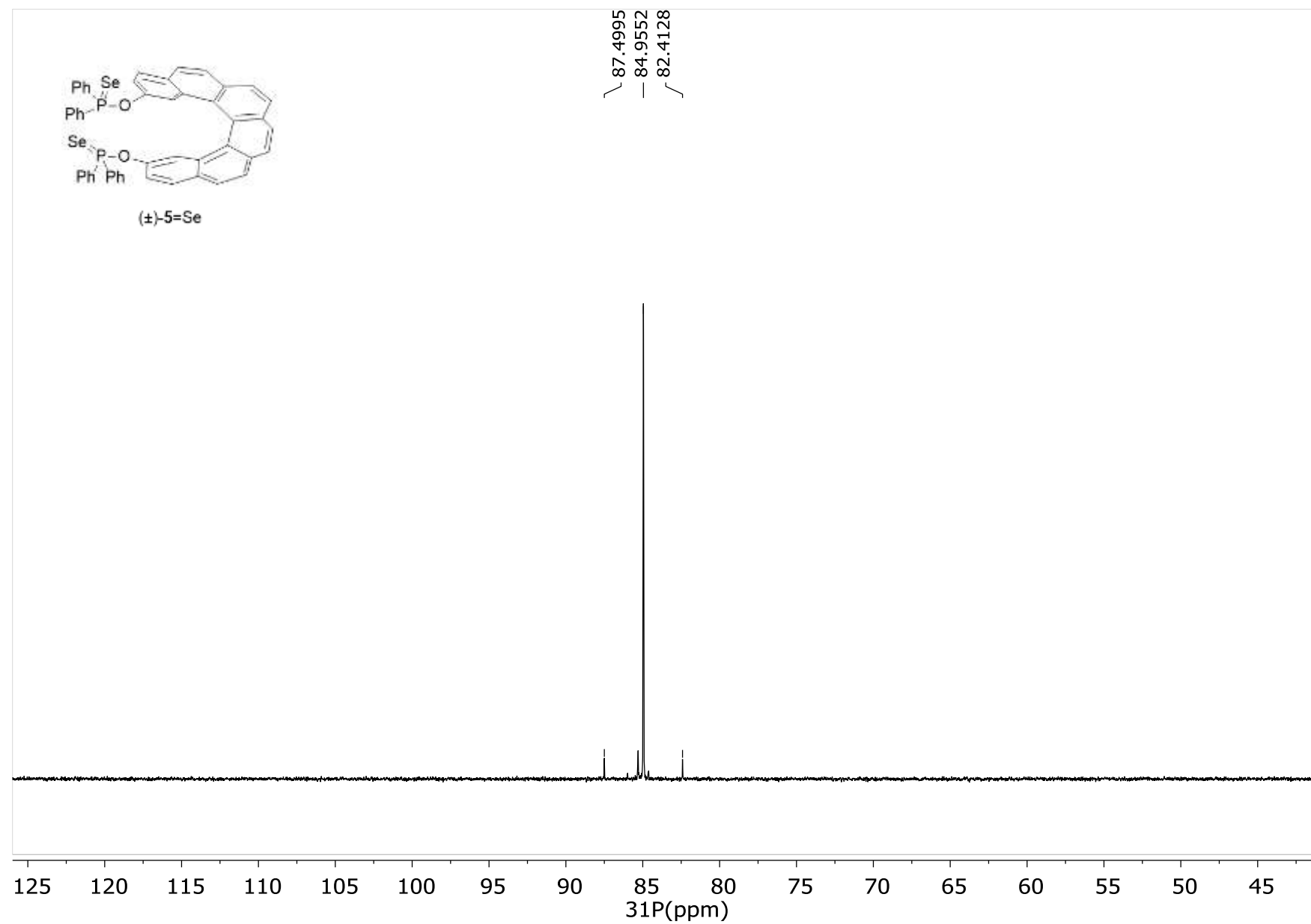


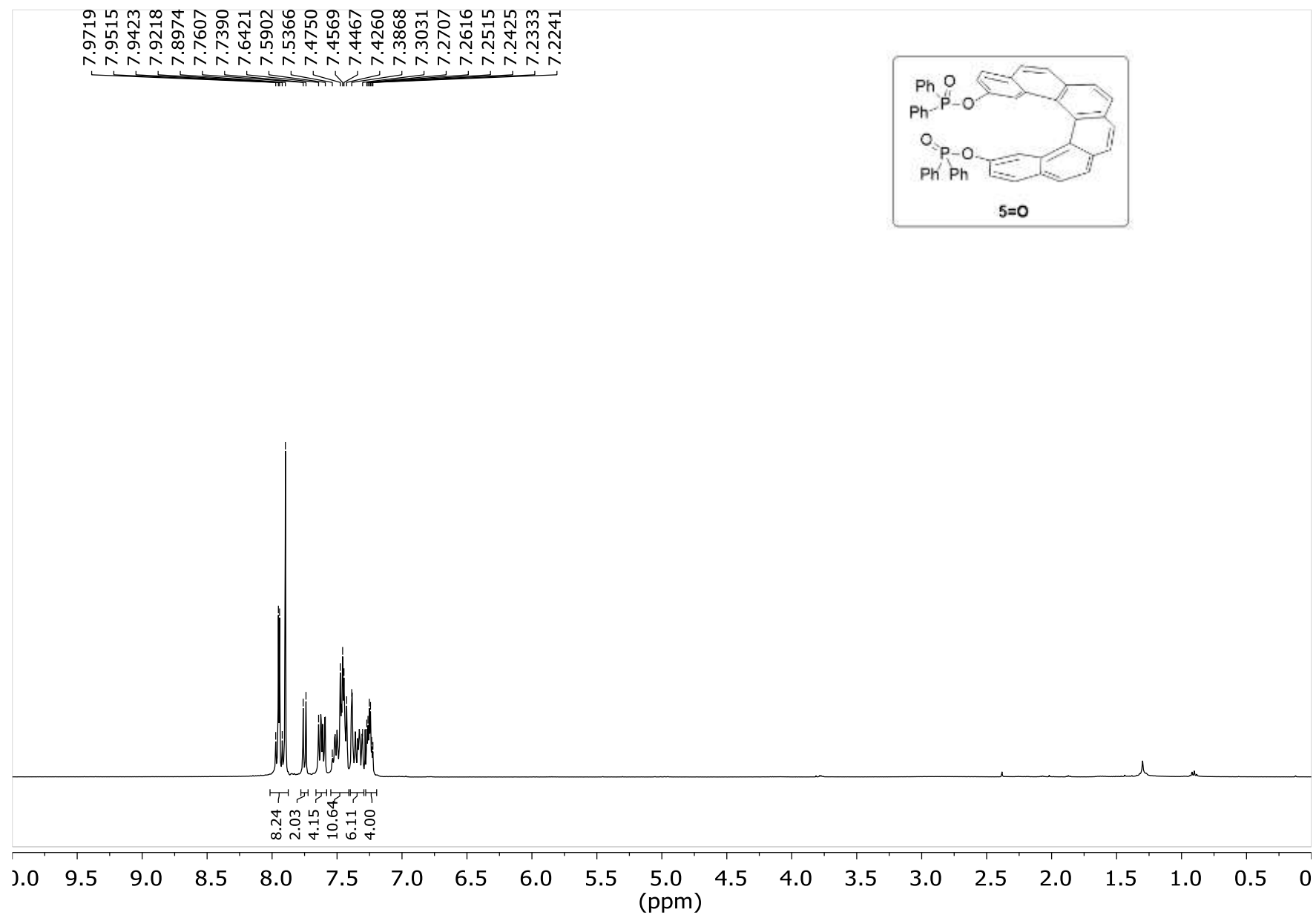


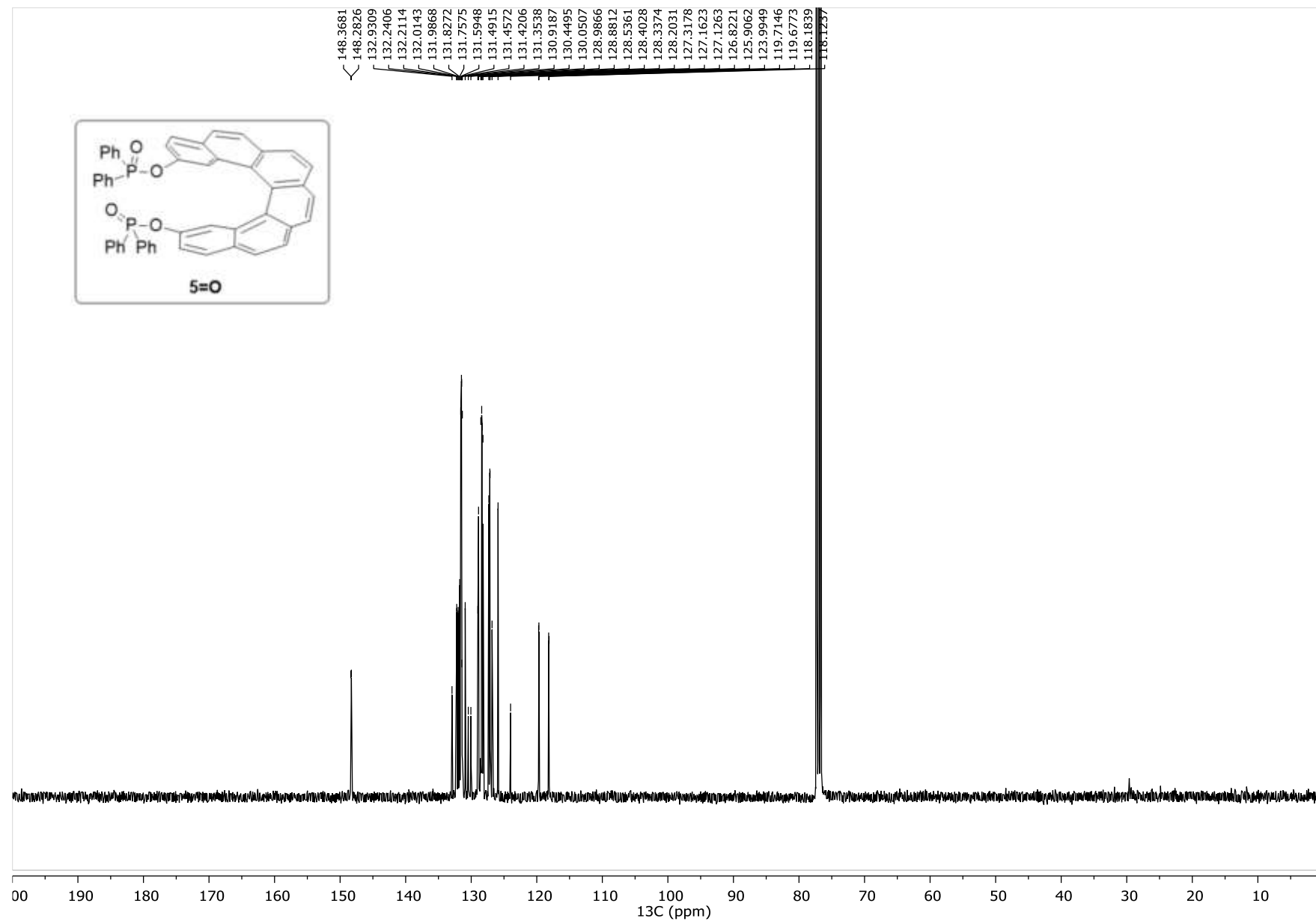
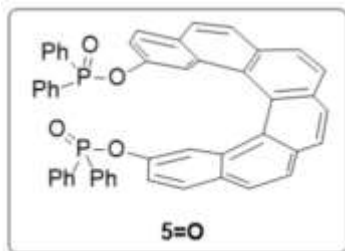


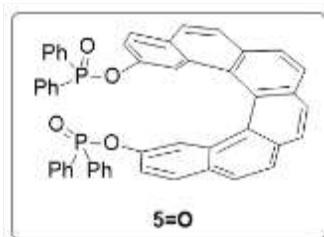


(±)-5=Se

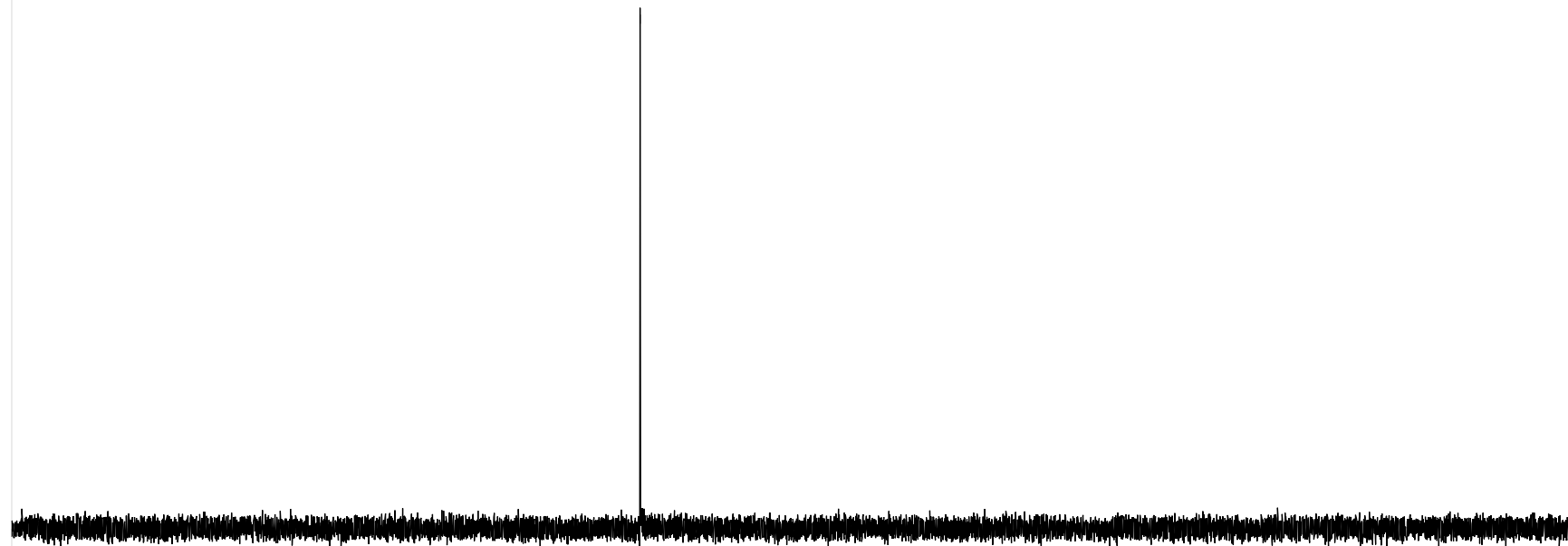




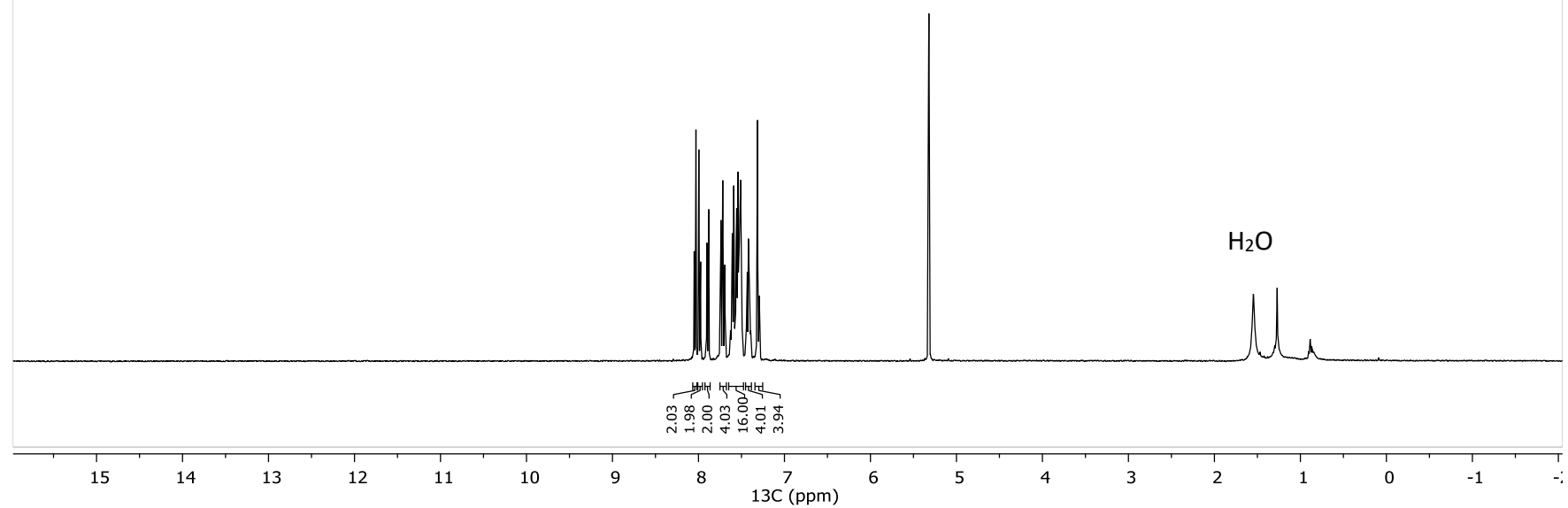
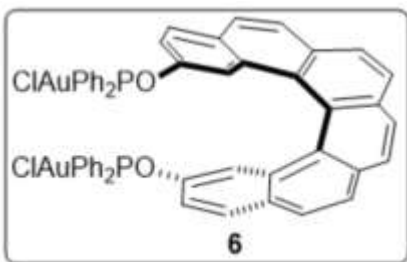


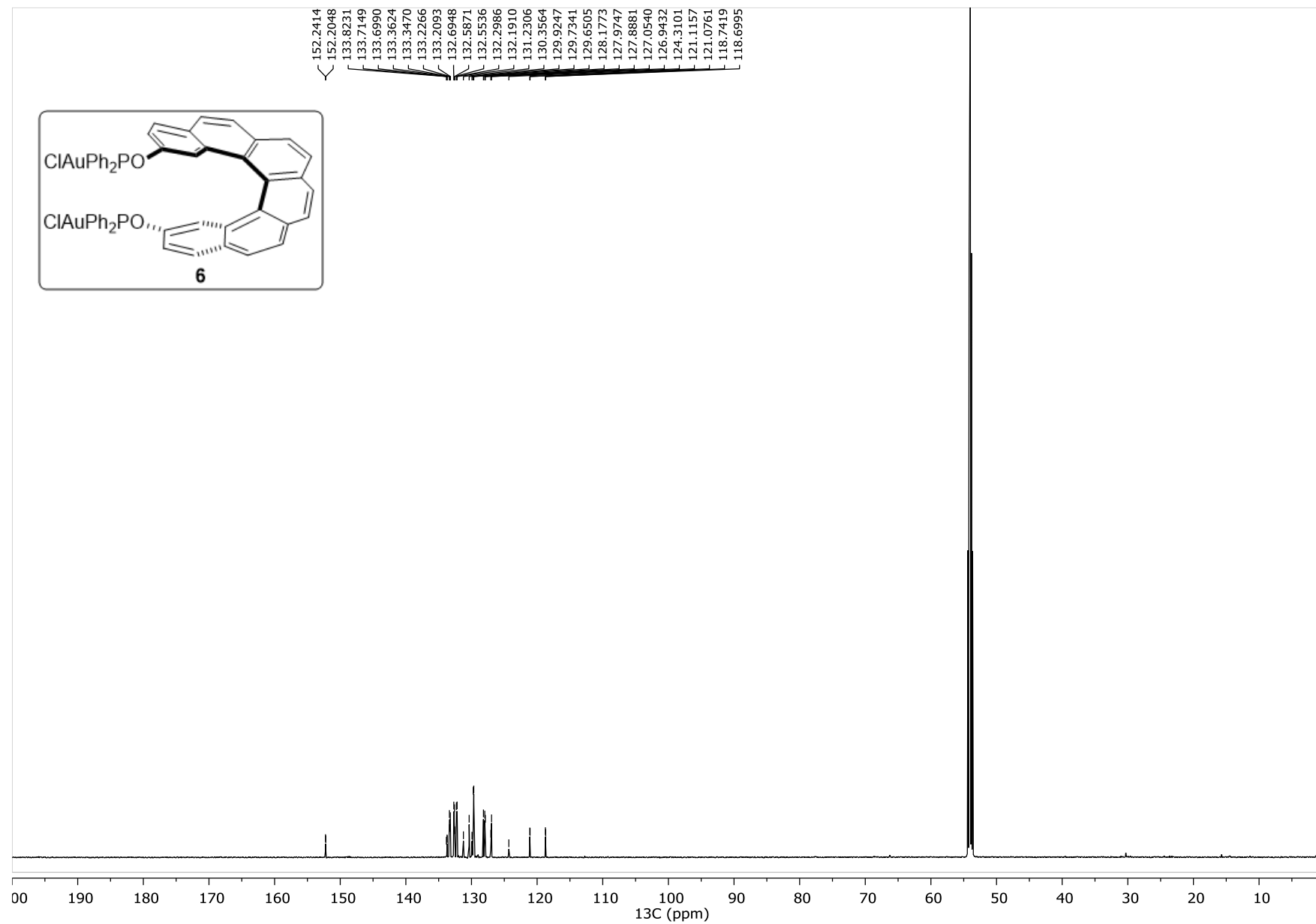
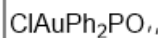


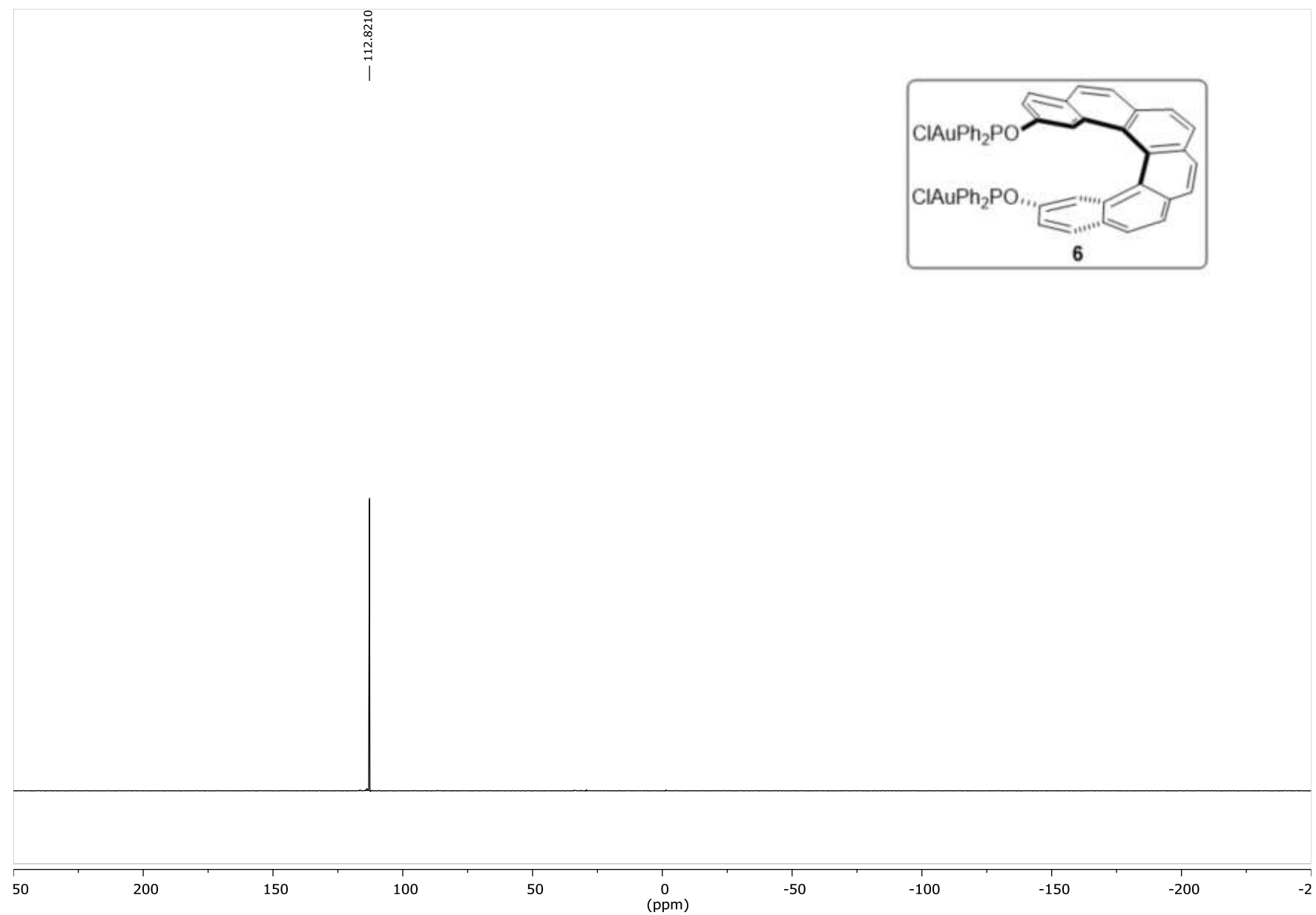
— 29.5702



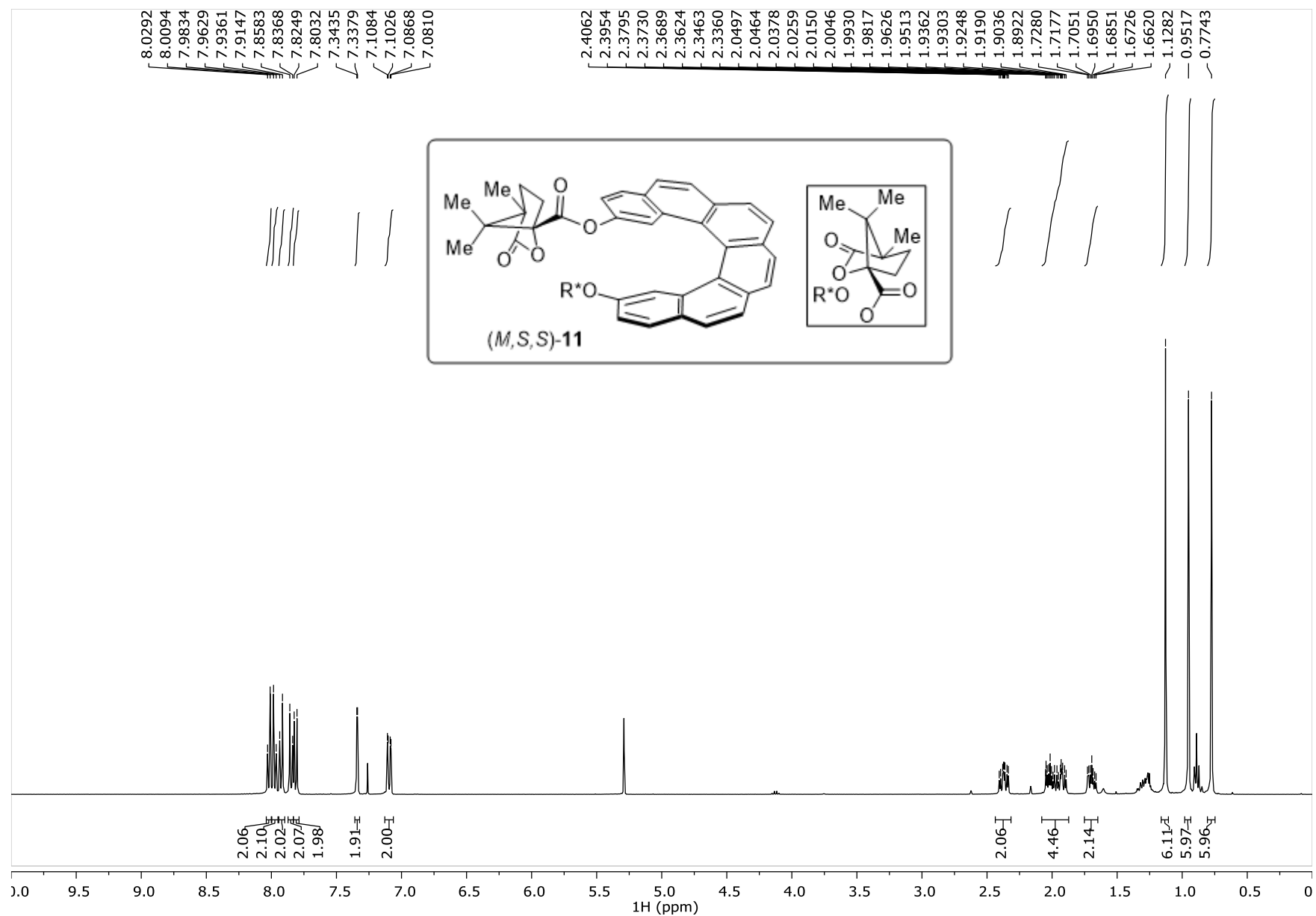
140 120 100 80 60 40 20 0 -20 -40 -60 -80 -100 -120 -140  
 $^{31}\text{P}$  (ppm)

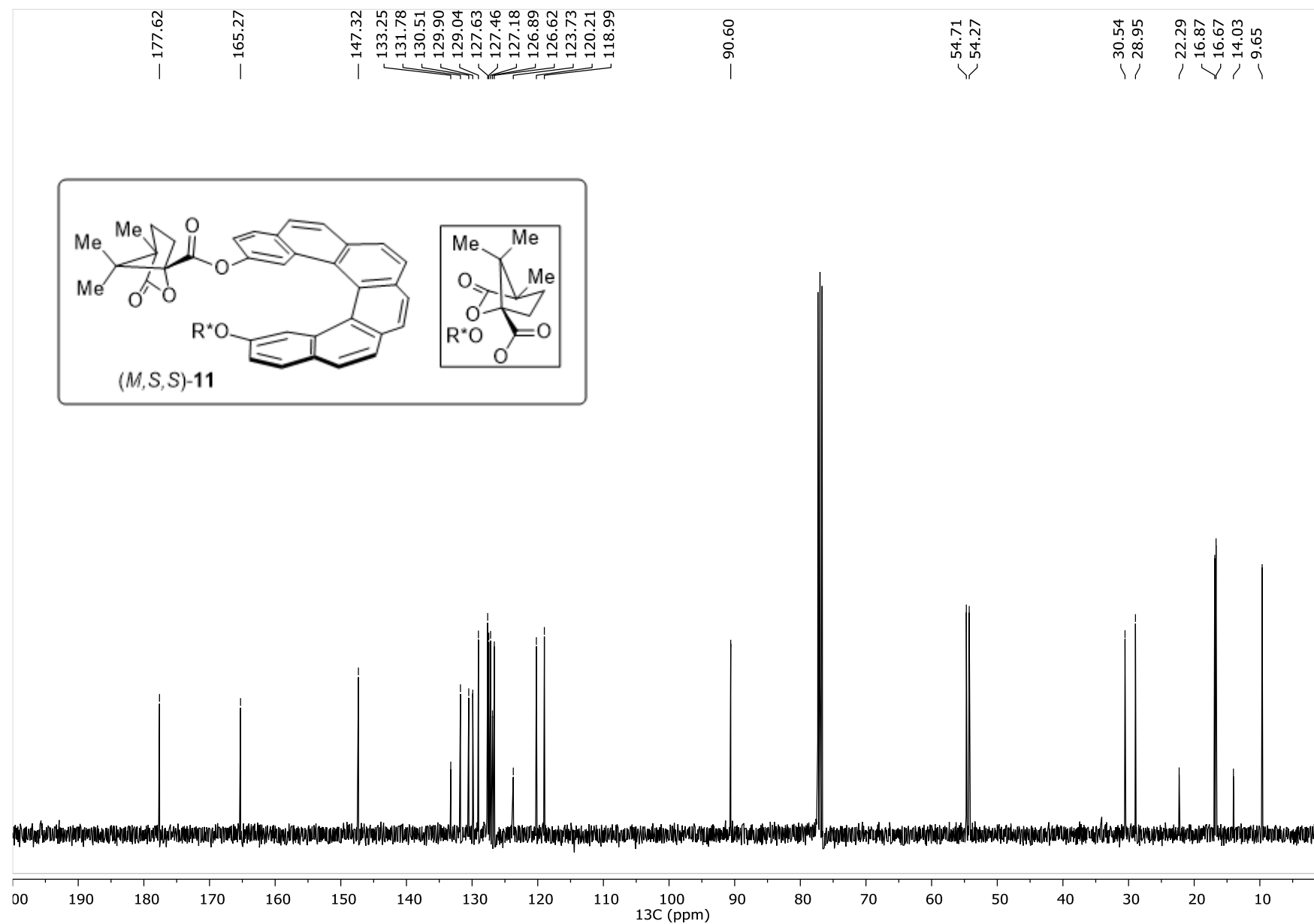


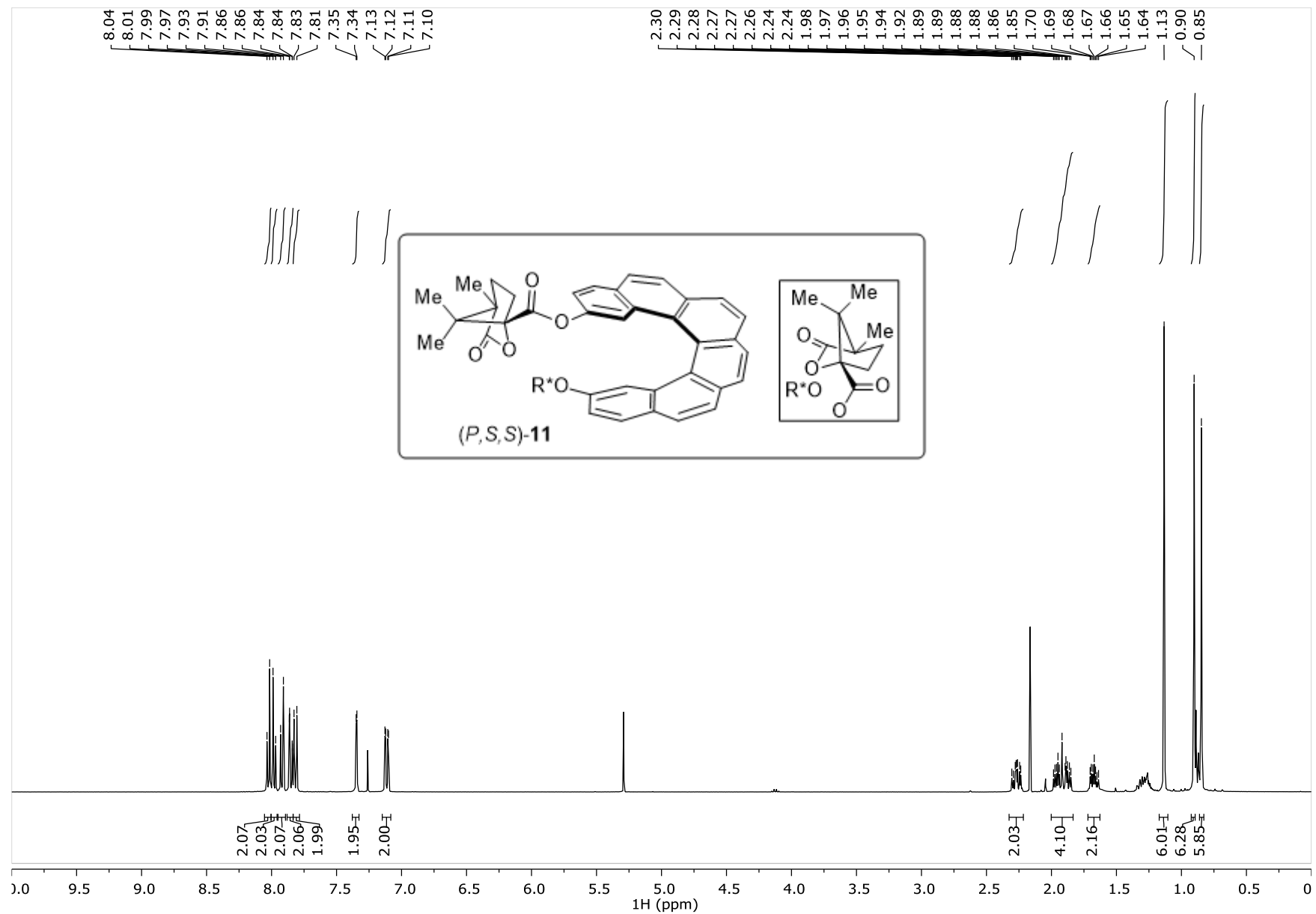


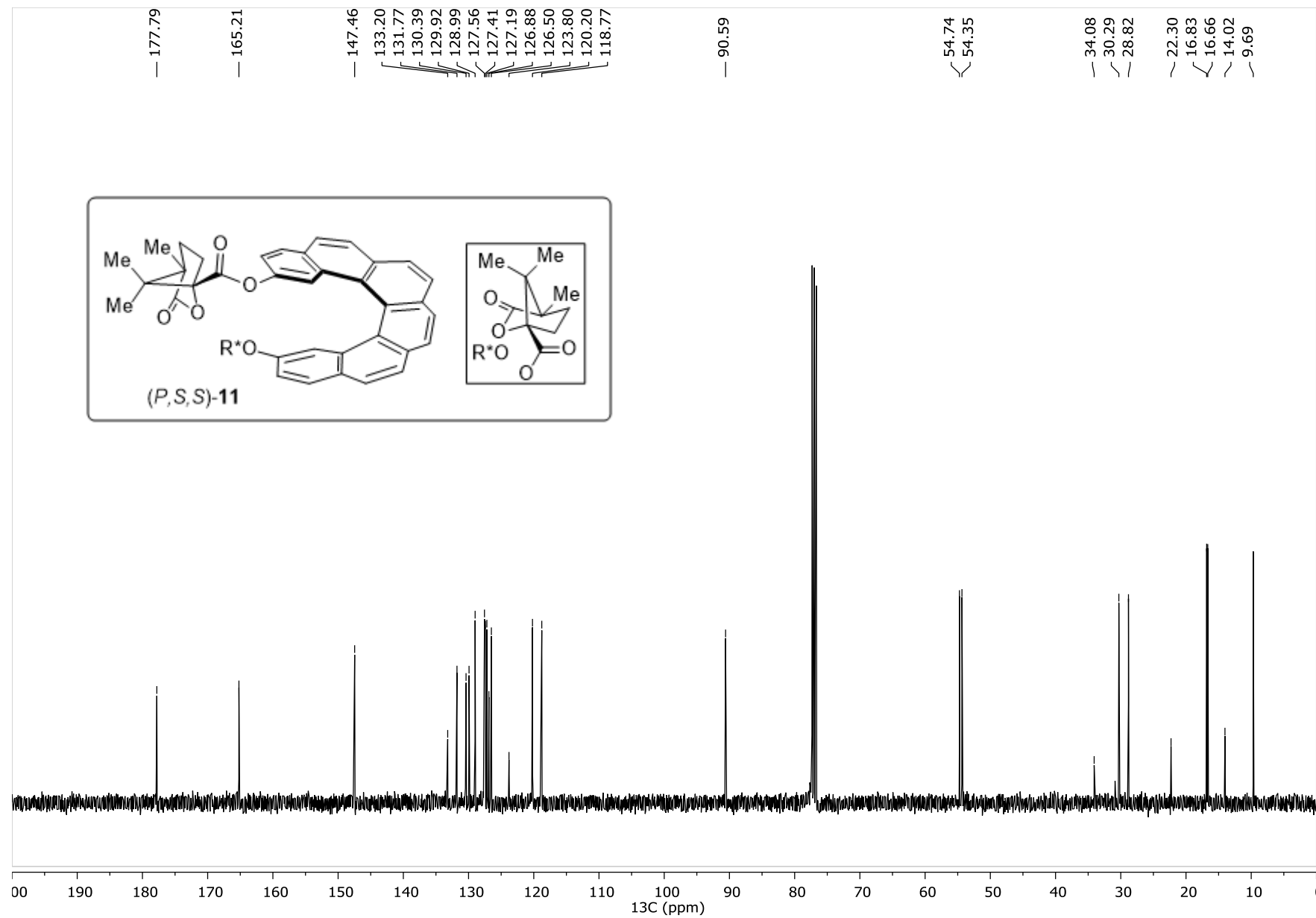




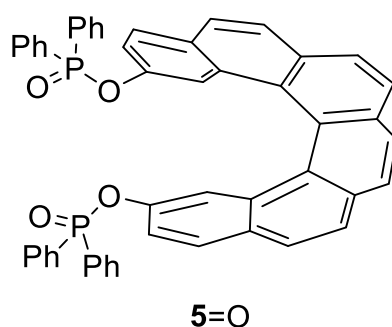






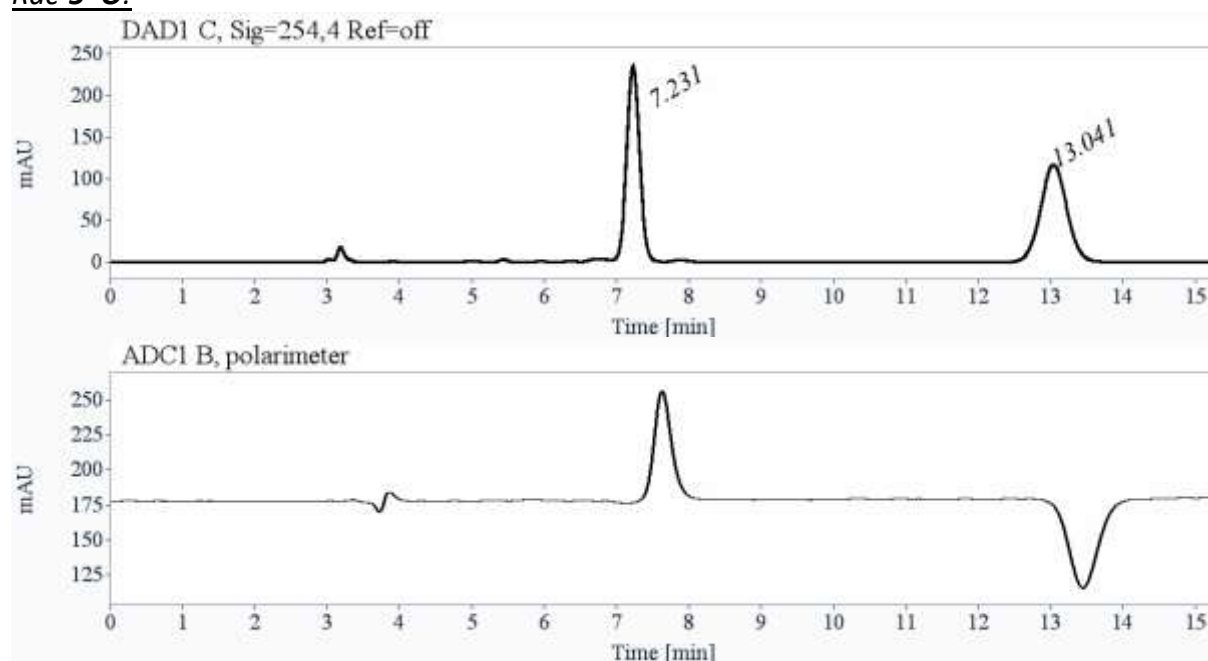


## 2. Chiral HPLC analysis for 5=O



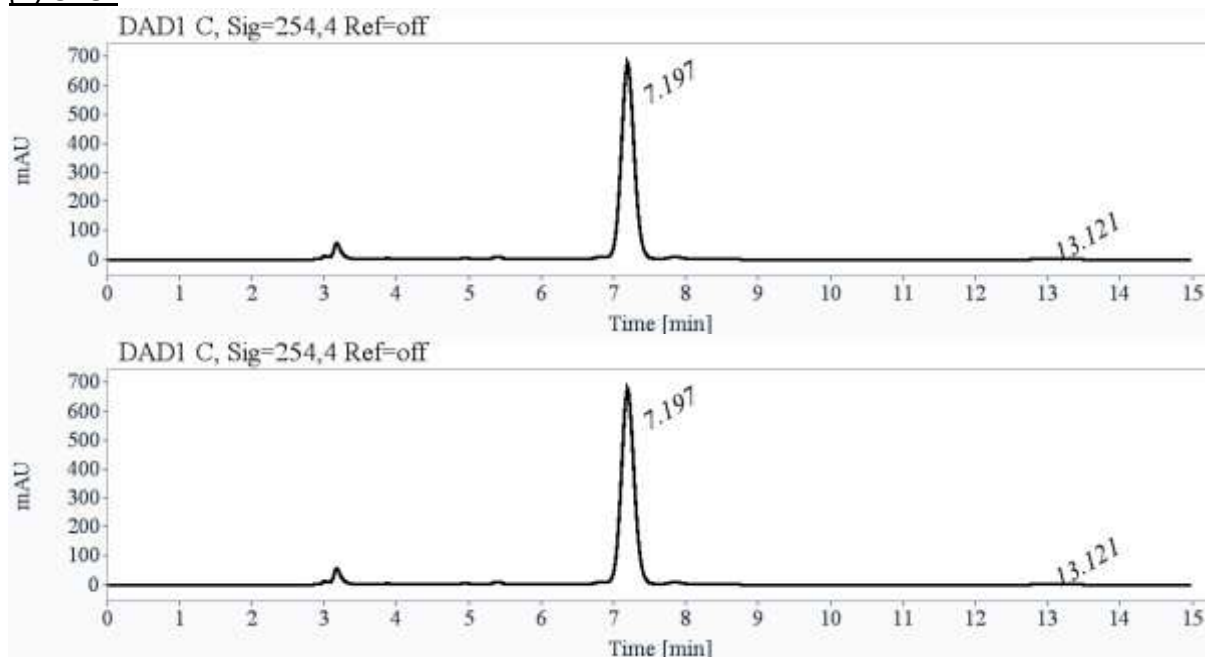
Conditions: Chiralpak IF (250 x 4.6 mm, 5 microns), amylose tris(3-chloro-4-methylphenylcarbamate) immobilized on silica, mobile phase : heptane / ethanol / dichloromethane (5/3/2), flow-rate = 1 mL/min, UV detection at 254 nm and polarimetric detection (Jasco OR-1590), Rt (*P*) = 7.2 min, Rt (*M*) = 13.0 min, k (*P*) = 1.4, k (*M*) = 3.4, enantioselectivity  $\alpha$  = 2.3 and resolution = 11.

### Rac-5=O:



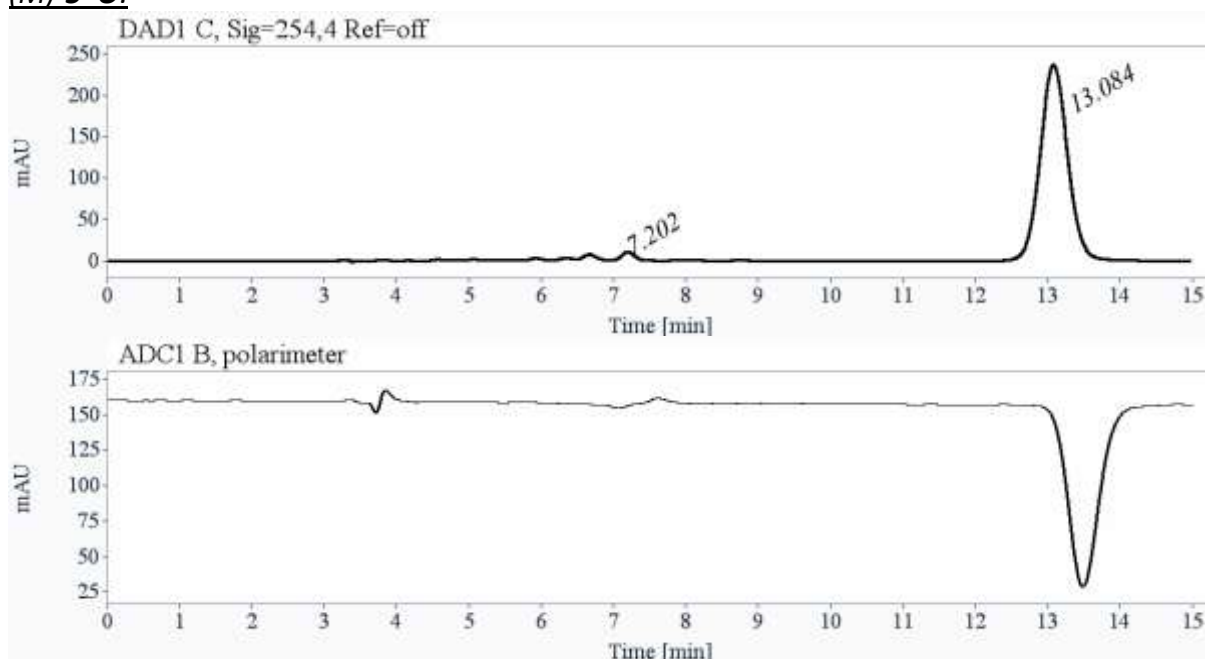
RT [min]	Area	Area%	Capacity Factor	Enantioselectivity	Resolution (USP)
7.23	2942	49.28	1.45		
13.04	3028	50.72	3.42	2.36	11.57
Sum	5969	100.00			

(P)-5=0:



RT [min]	Area	Area%
7.20	8648	99.14
13.12	75	0.86
Sum	8723	100.00

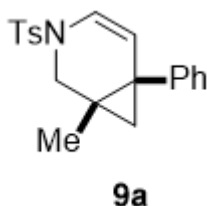
(M)-5=0:



RT [min]	Area	Area%
7.20	125	1.96
13.08	6282	98.04
Sum	6407	100.00

### 3. ASYMMETRIC CATALYSIS

#### Chiral HPLC analysis for **9a**



Two different analytical conditions were used to determine and confirm the low enantiomeric excesses.

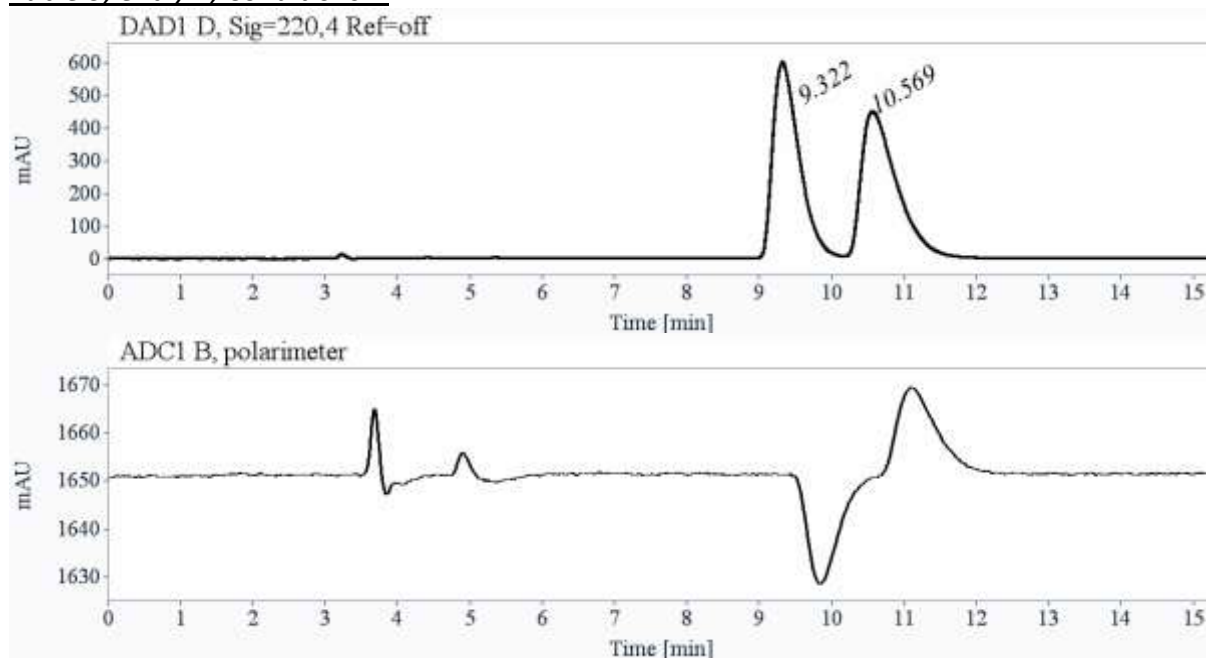
#### Conditions A:

Chiralpak AS-H (250 x 4.6 mm, 5 microns), amylose tris[(*S*)alpha-phenethyl] carbamate coated on silica, mobile phase : heptane / 2-PrOH (95/5), flow-rate = 1 mL/min, UV detection at 220 nm and polarimetric detection (Jasco OR-1590),  $R_t$  (*R,R*) = 9.3 min,  $R_t$  (*S,S*) = 10.6 min,  $k$  (*R,R*) = 2.2,  $R_t$  (*S,S*) = 2.6, enantioselectivity  $\alpha$  = 1.18 and resolution = 1.6.

#### Conditions B:

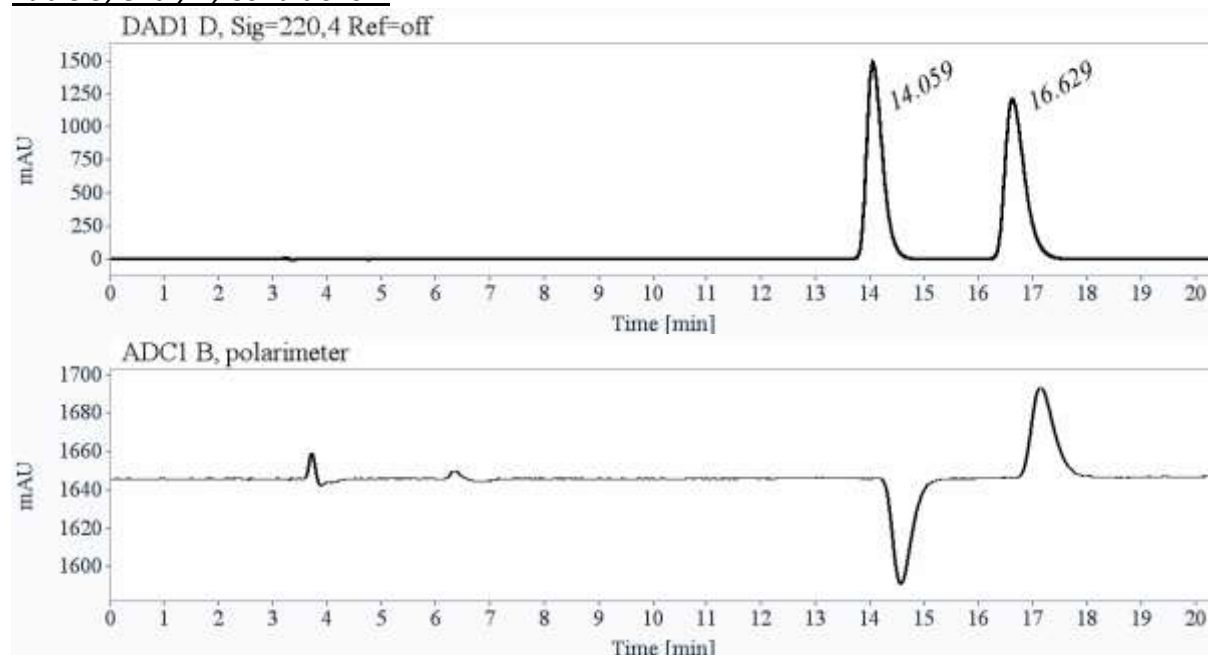
Lux-Cellulose-4 (250 x 4.6 mm, 3 microns), Cellulose tris(4-chloro-3-methylphenylcarbamate) coated on silica, mobile phase : heptane / 2-PrOH (95/5), flow-rate = 1 mL/min, UV detection at 220 nm and polarimetric detection (Jasco OR-1590),  $R_t$  (*R,R*) = 14.0 min,  $R_t$  (*S,S*) = 16.6 min,  $k$  (*R,R*) = 3.8,  $R_t$  (*S,S*) = 4.7, enantioselectivity  $\alpha$  = 1.23 and resolution = 4.3.

Table 5, entry 1, Conditions A



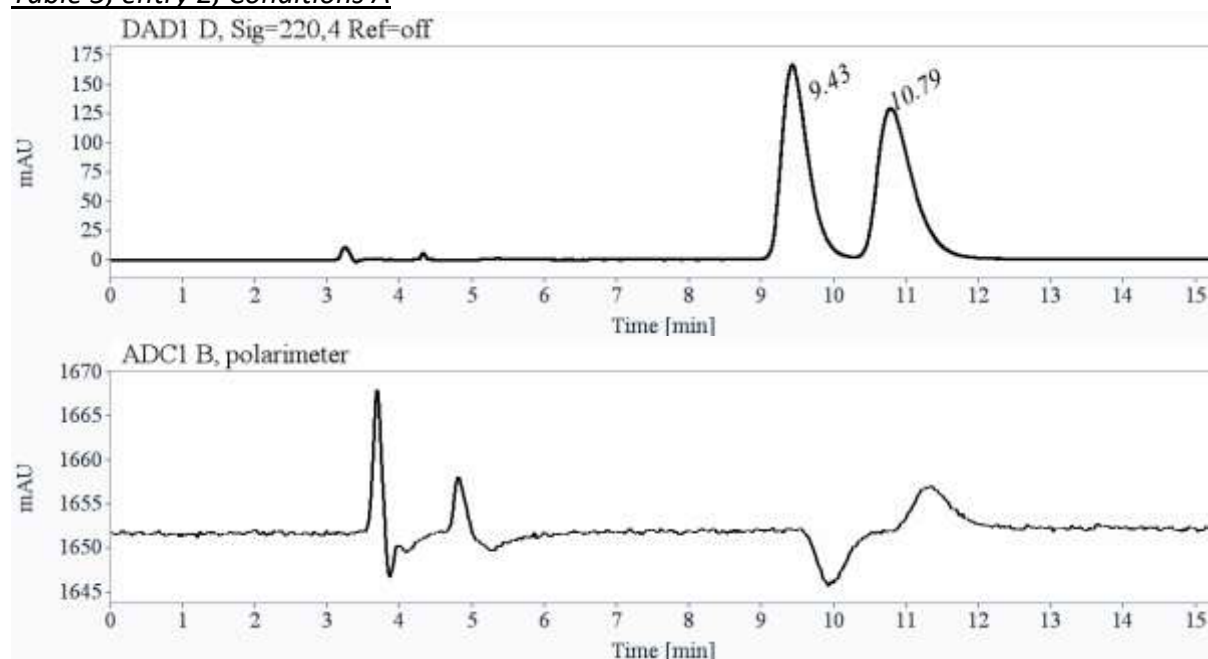
RT [min]	Area	Area%
9.32	15324	49.64
10.57	15543	50.36
Sum	30867	100.00

**Table 5, entry 1, Conditions B**



RT [min]	Area	Area%
14.06	30287	49.77
16.63	30569	50.23
Sum	60856	100.00

**Table 5, entry 2, Conditions A**



RT [min]	Area	Area%
9.43	4256	48.66
10.79	4490	51.34
Sum	8747	100.00



Table 5, entry 2, Conditions B

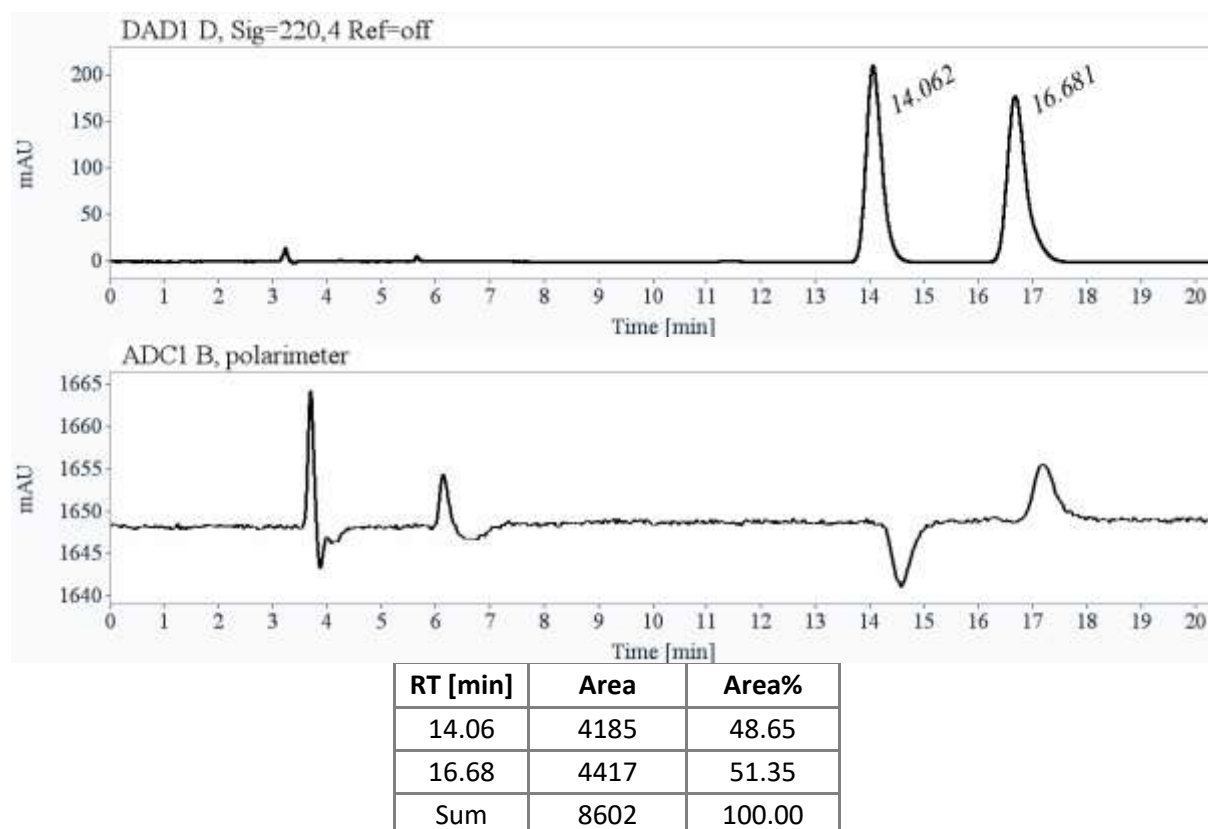


Table 5, entry 3, Conditions A

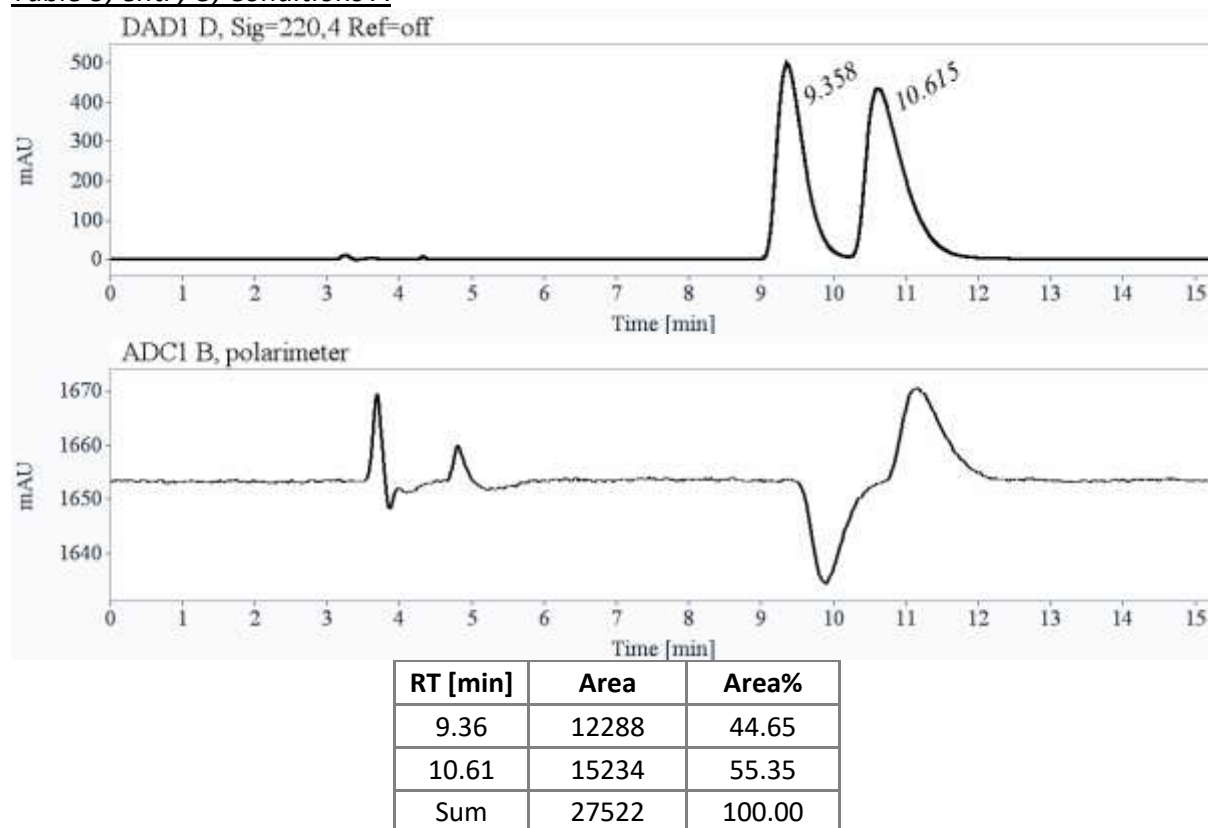
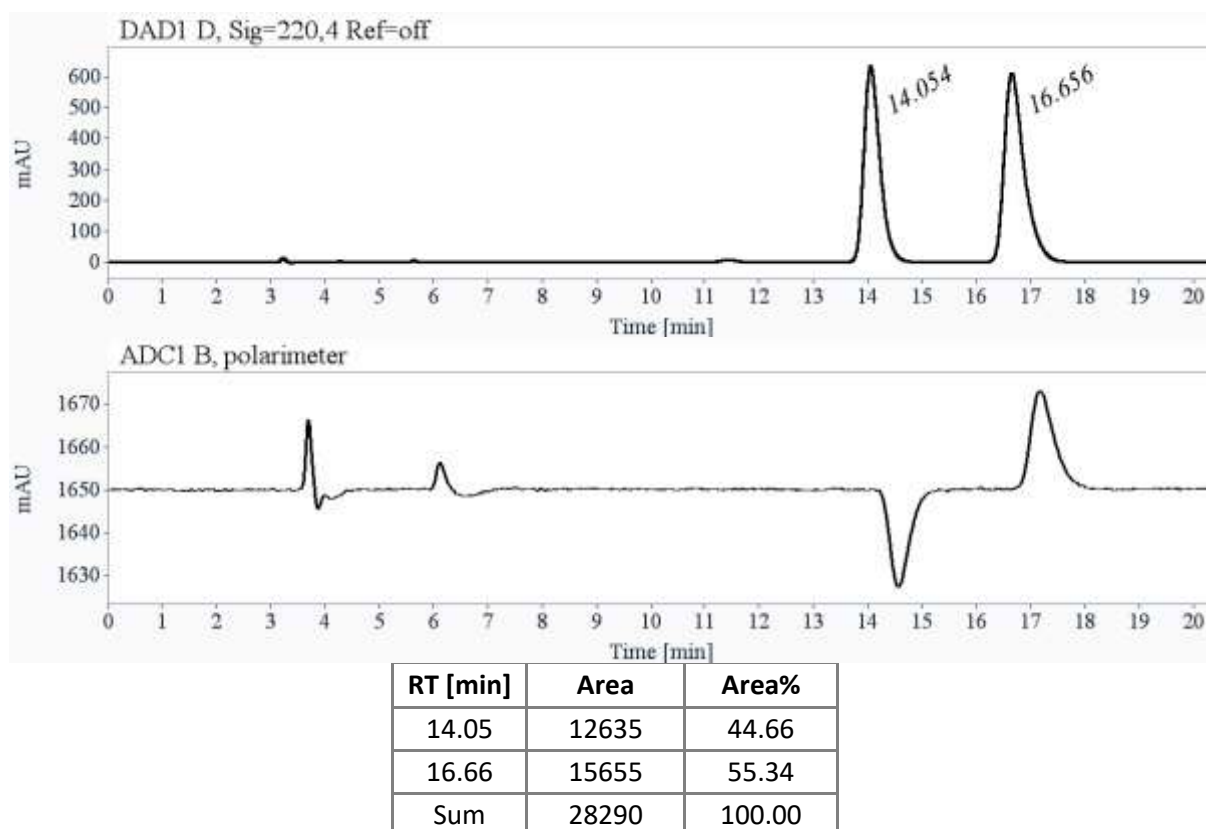
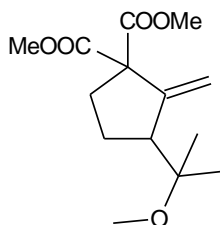


Table 5, entry 3, Conditions B



Chiral HPLC analysis for **12e**

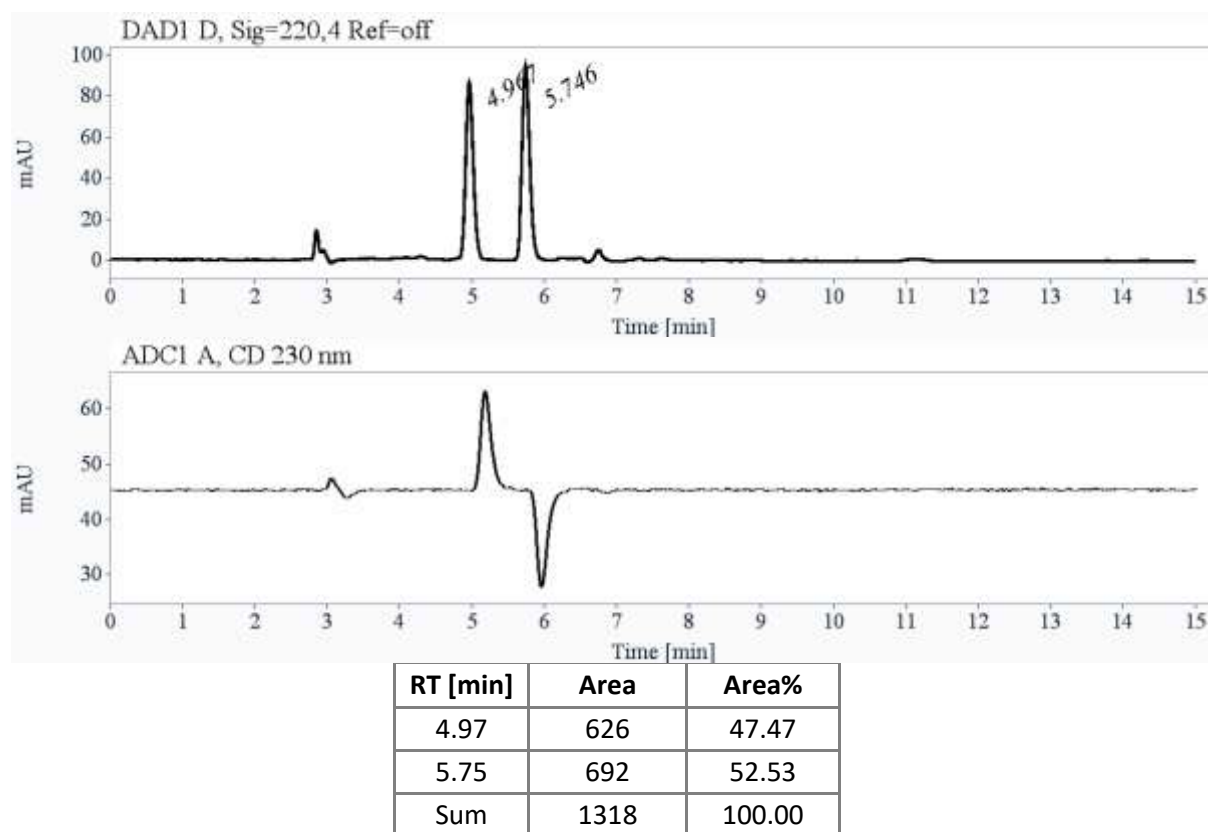


Two different analytical conditions were used to determine and confirm the low enantiomeric excesses.

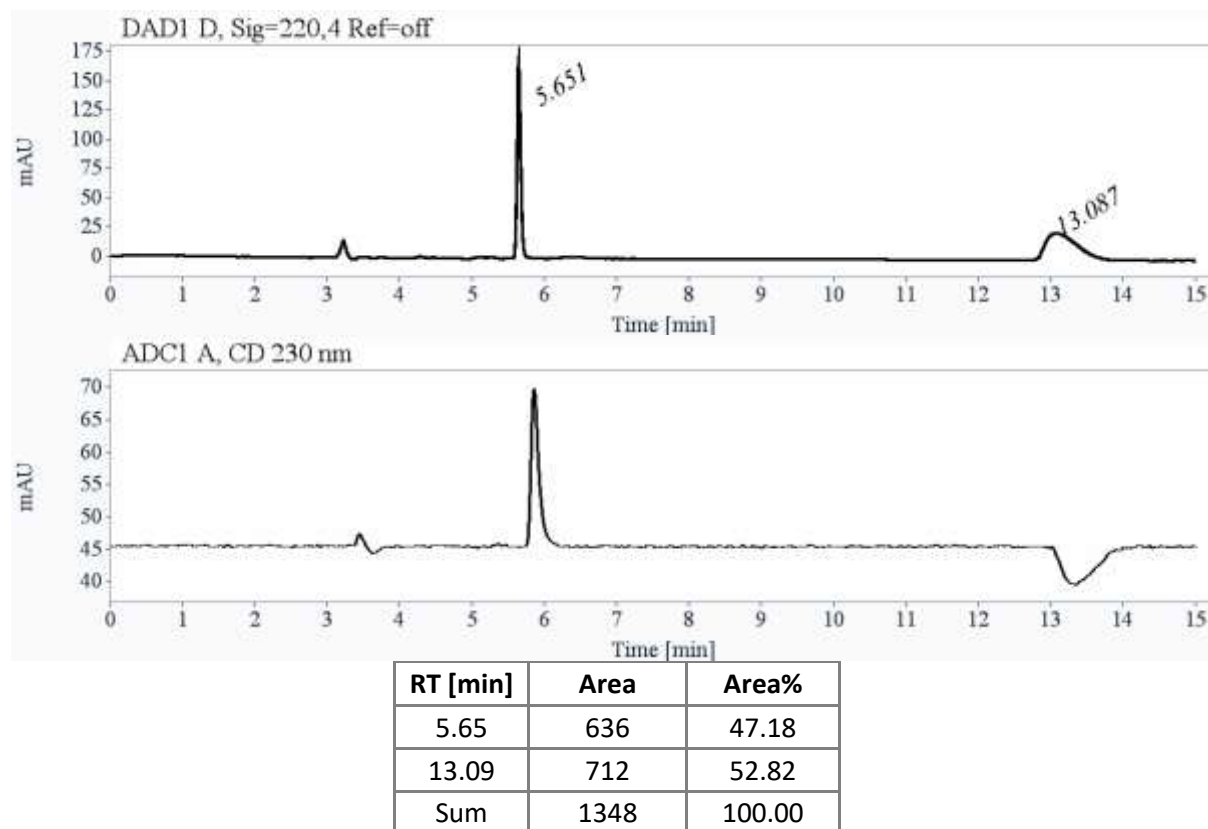
**Conditions A:** Lux-Amylose-1 (250 x 4.6 mm, 5 microns), amylose tris(3,5-dimethylphenylcarbamate) coated on silica, mobile phase : heptane / 2-PrOH (95/5), flow-rate = 1 mL/min, UV detection at 220 nm and circular dichroism detection at 230 nm (Jasco CD-2095), Rt (S) = 5.0 min, Rt (R) = 5.7 min, k (S) = 0.7, Rt (R) = 0.9, enantioselectivity  $\alpha$  = 1.3 and resolution = 4.

**Conditions B:** Lux-Cellulose-4 (250 x 4.6 mm, 3 microns), Cellulose tris(4-chloro-3-methylphenylcarbamate) coated on silica, mobile phase : heptane / 2-PrOH (95/5), flow-rate = 1 mL/min, UV detection at 220 nm and circular dichroism detection at 230 nm (Jasco CD-2095), Rt (S) = 5.7 min, Rt (R) = 13.0 min, k (S) = 0.9, Rt (R) = 3.4, enantioselectivity  $\alpha$  = 3.7 and resolution = 16.

### Scheme 5, Conditions A



### Scheme 5, Conditions B



## 4. CYCLOISOMERIZATION SPECTRA

